24. Ho AY, Pagliuca A, Kenyon M, et al. Reduced-intensity allogeneic hematopoietic stem cell transplantation for myelodysplastic syndrome and acute myeloid leukemia with multilineage dysplasia using fludarabine, busulphan, and alemtuzumab (FBC) conditioning. *Blood*. 2004;104:1616-1623.
25. van Besien K, Artz A, Smith S, et al. Fludarabine, melphalan, and alemtuzumab conditioning in adults with standard-risk advanced acute myeloid leukemia and myelodysplastic syndrome. *J Clin Oncol*. 2005;23:5728-5738.
26. Lim ZY, Ho AY, Ingram W, et al. Outcomes of alemtuzumab-based reduced intensity conditioning stem cell transplantation using unrelated donors for myelodysplastic syndromes. *Br J Haematol*. 2006;135:201-209.
27. de Lima M, Couriel D, Thall PF, et al. Once-daily intravenous busulfan and fludarabine: clinical and pharmacokinetic results of a myeloablative, reduced-toxicity conditioning regimen for allogeneic stem cell transplantation in AML and MDS. *Blood*. 2004;104:857-864.

IMMUNOLOGY ORIGINAL ARTICLE

Interleukin (IL)-4 promotes T helper type 2-biased natural killer T (NKT) cell expansion, which is regulated by NKT cell-derived interferon-γ and IL-4

Akira Iizuka,[1,4,5] Yoshinori Ikarashi,[1] Mitsuzi Yoshida,[1] Yuji Heike,[5] Kazuyoshi Takeda,[6] Gary Quinn,[3] Hiro Wakasugi,[2] Masanobu Kitagawa[4] and Yoichi Takaue[5]

[1]*Chemotherapy and* [2]*Pharmacology Divisions, and* [3]*Section for Studies on Metastasis, National Cancer Center Research Institute,* [4]*Department of Comprehensive Pathology, Aging and Developmental Sciences, Tokyo Medical and Dental University, Graduate School,* [5]*Hematopoietic Stem Cell Transplantation/Immunotherapy Unit, National Cancer Center Hospital, and* [6]*Department of Immunology, Juntendo University School of Medicine, Tokyo, Japan*

doi:10.1111/j.1365-2567.2007.02732.x
Received 31 January 2007; revised 20 August 2007; accepted 4 September 2007.
Correspondence: Dr Y. Ikarashi, Chemotherapy Division, National Cancer Center Research Institute, 5-1-1, Tsukiji, Chuo-ku, Tokyo 104-0045, Japan.
Email: yikarash@gan2.ncc.go.jp
Senior author: Dr Y. Ikarashi

Summary

CD1d-restricted natural killer T (NKT) cells can rapidly produce T helper type 1 (Th1) and Th2 cytokines and also play regulatory or pathological roles in immune responses. NKT cells are able to expand when cultured with α-galactosylceramide (α-GalCer) and interleukin (IL)-2 in a CD1d-restricted manner. However, the expansion ratio of human NKT cells is variable from sample to sample. In this study, we sought to determine what factor or factors are responsible for efficient *in vitro* expansion of NKT cells from various inbred mouse strains. Although the proportion of NKT cells in the spleen was nearly identical in each mouse strain, the growth rates of NKT cells cultured *in vitro* with α-GalCer and IL-2 were highly variable. NKT cells from the B6C3F1 and BDF1 mouse strains expanded more than 20-fold after 4 days in culture. In contrast, NKT cells from the strain C3H/HeN did not proliferate at all. We found that cell expansion efficiency correlated with the level of IL-4 detectable in the supernatant after culture. Furthermore, we found that exogenous IL-4 augmented NKT cell proliferation early in the culture period, whereas interferon (IFN)-γ tended to inhibit NKT cell proliferation. Thus, the ratio of production of IL-4 and IFN-γ was important for NKT cell expansion but the absolute levels of these cytokines did not affect expansion. This finding suggests that effective expansion of NKT cells requires Th2-biased culture conditions.

Keywords: natural killer T cell; interleukin-4; interferon-γ; glycolipid

Introduction

Mouse natural killer T (NKT) cells were initially identified as a T-cell subset that expresses NK cell receptors such as NK1·1, CD94 and Ly49.[1,2] The majority of NKT cells have the invariant T-cell receptor (TCR) α-chain rearrangement Vα14-Jα18 and recognize antigens presented by CD1d, a non-classical major histocompatibility complex (MHC) class I molecule.[3,4] NKT cells are continuously sensitized by endogenous antigens so that they display an effector-memory phenotype (such as $CD62L^{low}$ $CD44^{high}$)[5–7] and rapidly produce large amounts of T helper type 1 (Th1) and Th2 cytokines when stimulated with lipid antigens such as α-galactosylceramide (α-GalCer) in a CD1d-dependent manner.[2,8] NKT cells are regarded as immunoregulatory because of their cytokine profile. Moreover, NKT cells are thought to play an important role in response to infectious agents and in pathological responses such as allergies or autoimmune disease. NKT cells are cytotoxic to various tumour cell lines via Fas-ligand-, tumour necrosis factor-related apoptosis-inducing ligand (TRAIL)- and/or perforin-dependent pathways,[9–12] and play a role in tumour surveillance.[13] NKT cells activated by interleukin (IL)-12 or α-GalCer sequentially activate natural killer (NK) cells by producing interferon (IFN)-γ and induce antitumour immune responses. This in turn inhibits tumour metastasis and can suppress solid tumour growth. In some studies, it has been suggested that this ability helps to induce tumour antigen-specific CD8 T cells, thereby making an additional contribution to the immune response to cancer.[14]

In humans, counterparts of mouse NKT cells have also been found to be responsive to α-GalCer, which induces them to secrete IL-4 and IFN-γ. In addition, they have been shown to be cytotoxic to tumour cells via two different mechanisms, a CD1d-dependent and a CD1d-independent mechanism.[15] Human NKT cells have the

potential to induce antitumour responses *in vivo*. However, in patients with malignancies,[16,17] NKT cells are reduced in number and activity, and *in vivo* activation by α-GalCer leads to transient activation and long-term unresponsiveness of NKT cells.[18,19] For that reason, adaptive transfer of *in vitro* expanded and/or activated NKT cells is expected to induce effective antitumour responses.

To date, several combinations of cytokines with α-GalCer have been reported to expand NKT cells isolated from peripheral mononuclear cells. However, NKT cells present a diverse range of expansion ratios even among healthy individuals.[20,21] Although a previous study suggested that differences in NKT cell proliferation are associated with the age of the donor,[22] there is still much that remains to be determined concerning additional factors that influence NKT cell proliferation.

In this study, we used inbred mouse strains as an experimental system in which to reveal factors that affect variation in proliferation rates among individuals. Previously, we found that *in vitro* expanded NKT cells from C57BL/6 mice retained an effector-memory-like phenotype and retained the ability to produce cytokines.[23] In addition, we found that there was a marked difference in the NKT cell expansion ratio among various mouse strains and that the differences were closely related to the bias in production of Th1 or Th2 cytokines by NKT cells. Finally, we report that a relatively low rate of proliferation can be enhanced by the addition of IL-4, which creates Th2-biased culture conditions.

Materials and methods

Mice

Female C57BL/6N, BALB/cA, C3H/HeN, DBA/2N (C57BL/6 × DBA/2)F_1 (BDF1), (C57BL/6 × C3H/HeN)F_1 (B6C3F1), and SJL/J mice were purchased from Charles River Japan (Kanagawa, Japan). All mice, which were maintained in our animal facilities, were 8–11 weeks of age at the time of the experiment. All animal protocols for this study were reviewed and approved by the committee for ethics of animal experimentation at the National Cancer Center of Japan prior to the beginning of the study.

Monoclonal antibodies and reagents

Anti-IL-4 (clone 11B11) and anti-IFN-γ (clone R4-6A2) monoclonal antigen-neutralizing antibodies (mAbs) were obtained from the supernatant of a hybridoma culture maintained in serum-free medium in a CELLine CL-1000 flask (BD Biosciences, San Jose, CA) and purified by Protein G Sepharose (GE Healthcare Amersham Biosciences AB, Uppsala, Sweden) affinity column chromatography. Anti-CD16/32 (clone 2·4G2) was obtained from a hybridoma supernatant. Fluorescein isothiocyanate (FITC)-conjugated anti-CD3 (clone 145-2C11), allophycocyanin (APC)-conjugated anti-IL-4 (11B11), anti-IFN-γ (XMG1·2), and a rat immunoglobulin G1 (IgG1) isotype control (clone R3-34) and Golgi Stop™ were obtained from BD Biosciences. α-Galactosylceramide (α-GalCer) was kindly provided by the Pharmaceutical Research Laboratory, KIRIN Brewery Co., Ltd (Gunma, Japan). The phycoerythrin (PE)-conjugated CD1d/α-GalCer tetramer was prepared using a baculovirus expression system as previously described.[24] Human recombinant IL-2 (rIL-2) was kindly provided by Takeda Chemical Industries Ltd (Osaka, Japan). Mouse rIL-4 was obtained from PeproTech EC Ltd (London, UK).

Flow cytometry

NKT cells were detected by multicolour flow cytometry as previously described.[23] Briefly, cells were preincubated with anti-CD16/32 mAb to block non-specific FcRγ binding and then stained with FITC-conjugated anti-CD3 and PE-conjugated CD1d/α-GalCer tetramer. Dead cells were excluded by propidium iodide staining and electronic gating. For detection of intracellular cytokines, cells were stimulated for 3 hr with phorbol 12-myristate 13-acetate (PMA) (25 ng/ml) and ionomycin (1 μg/ml), with the last 1 hr of stimulation in the presence of Golgi block, in a 37°, 5% CO_2 incubator, and then washed and incubated with anti-CD16/32 mAb, followed by incubation with FITC-conjugated anti-CD3 and PE-conjugated CD1d/α-GalCer tetramer. Cells were then permeabilized using Cytofix/Cytoperm (BD Biosciences) and IL-4 or IFN-γ was detected using APC-conjugated mAbs. Cells were analysed by flow cytometry (FACSCalibur; BD Biosciences).

NKT cell proliferation assay

Preparation of splenic mononuclear cells and *in vitro* expansion of NKT cells were performed as previously described.[23] Briefly, spleens of each mouse strain were macerated aseptically and pushed through a nylon mesh to obtain single-cell suspensions, and erythrocytes were lysed in ammonium chloride buffer. Mononuclear cells (1×10^6 cells/ml) were cultured with α-GalCer (50 ng/ml) and rIL-2 (100 IU/ml) in RPMI-1640 culture medium (Sigma-Aldrich, St. Louis, MO) supplemented with 8% fetal calf serum (JRH Biosciences, Lenexa, KS), 2-mercaptoethanol (5×10^{-5} M) 100 U/ml penicillin and 100 μg/ml streptomycin for 4 days in a 37°, 5% CO_2 incubator. After 4 days in culture, the absolute number of living cells was counted using a microscope after staining of cells with 0·2% trypan blue, and the relative percentages of NKT cells were determined by flow cytometry.

Cytokine production

The cell culture supernatant was collected after 24 hr or 4 days in culture and stored at −20°. The concentrations

of IL-4 and IFN-γ were determined by enzyme-linked immunosorbent assay (ELISA) (OptEIA ELISA set; BD Biosciences).

Results

α-GalCer-induced expansion of NKT cells from various mouse strains

Mouse NKT cells show a similar variation in expansion ratios to that observed for human NKT cells. We found that the expansion ratios were different for different mouse strains (Fig. 1). Before culture, spleen cell suspensions contained a small percentage (0·8–1·5%) and a small number (7–18 × 10^3 cells/ml) of NKT cells in each mouse strain. As shown in Fig. 1, culture of spleen cells with α-GalCer and IL-2 induced expansion of NKT cells, except for C3H/HeN mice. After 4 days of culture, NKT cells constituted 6·4–40·7% of cells in the culture and had expanded 7–25-fold in BALB/c, C57BL/6, DBA/2, B6C3F1 and BDF1 mice. The CD1d-restricted TCR α-chain Vα14 dominantly associates with the high-affinity TCR β-chain Vβ8·2, or the lower affinity chain Vβ8·3, Vβ7 or Vβ2, and a genetic defect in Vβ8 is reportedly the cause of the low responsiveness of NKT cells. We next asked if the TCR-β status of NKT cells had an effect on expansion. However, we found no significant differences among the six strains that were tested, and selective proliferation did not occur (data not shown).

NKT cell proliferation ratio correlates with amount of IL-4 in supernatant from a 4-day culture

Previously, a high concentration of IL-4 and IFN-γ in supernatant from a 4-day culture was observed.[23] Firstly, we measure amounts of IL-4 and IFN-γ in the culture supernatant.

An increase in the number of NKT cells was positively correlated with the production of IL-4 in the 4-day culture (Fig. 2a). However, high levels of IFN-γ were observed in all of the mouse strains, independent of an increase in either NKT cell number or IL-4 production. Almost all CD8 T cells acquired the ability to produce IFN-γ when activated indirectly via NKT cells by α-GalCer (data not shown), so it appears that, in C3H/HeN mice, NKT cells do not proliferate. Instead, it seems reasonable that a large amount of IFN-γ might be produced by the activated NK cells and CD8 T cells.[25,26]

A previous study reported cytokine secretion of NKT cells prior to their proliferation.[2,27] Thus, we harvested culture supernatants at 24 hr, before NKT cell expansion,[27] to determine the status of cytokine production at this early stage, which is the stage at which NKT cells initially respond to culture and initiate production of IL-4. This initial response positively correlated with NKT cell expansion to some degree, although the response was weaker than that observed for cells in culture for 4 days. It is notable that IL-4 production by C3H/HeN was more robust than that observed for C57BL/6, and IFN-γ

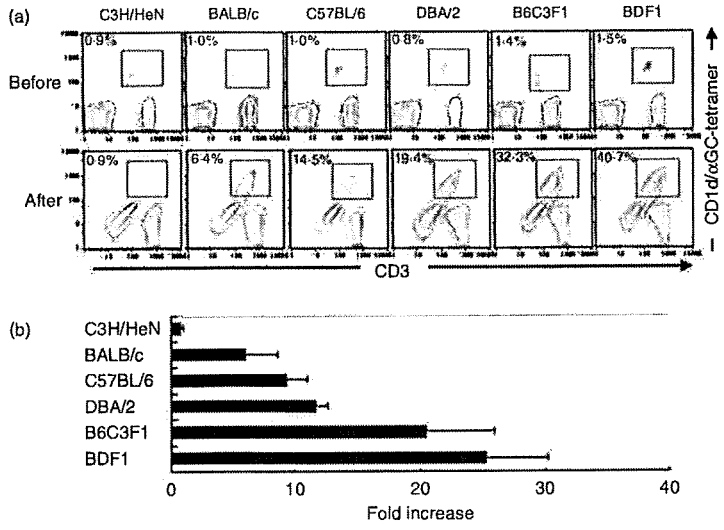

Figure 1. Expansion of natural killer T (NKT) cells *in vitro*. (a) Mouse spleen cells (1 × 10^6 cells/ml) were cultured with 50 ng/ml α-galactosylceramide (α-GalCer) and 100 U/ml interleukin (IL)-2 for 4 days. Cells were stained with anti-CD3 monoclonal antibody (mAb) and CD1d/α-GalCer tetramer and analysed by flow cytometry. The percentage of NKT cells was determined for both fresh (upper row) and cultured (lower row) cells. Representative results from replicate experiments are shown. (b) The fold increase in NKT cells after culture was calculated based on living cell counts and the percentage of NKT cells in the total cell population. Data are shown as mean ± standard error of the mean (n = 9 for C3H/HeN, BALB/c and C57BL/6; n = 4 for DBA/2, B6C3F1 and BDF1).

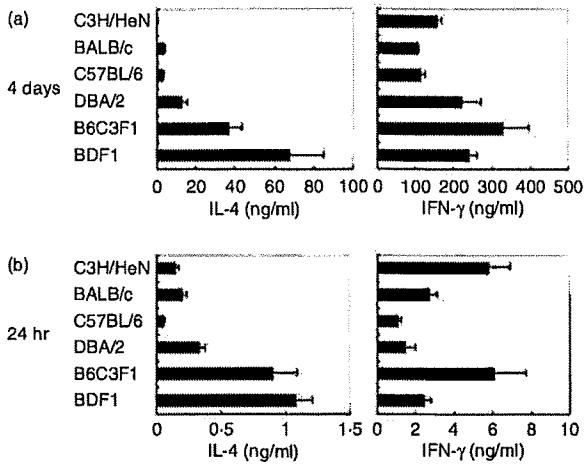

Figure 2. Production of interleukin (IL)-4 and interferon (IFN)-γ in expansion cell culture supernatants. Mouse spleen cells (1×10^6 cells/ml) were cultured with 50 ng/ml α-galactosylceramide (α-GalCer) and 100 U/ml IL-2 for 4 days. Supernatants were collected after 24 hr (b) or 4 days (a). The levels of IFN-γ and IL-4 in the supernatants were determined by enzyme-linked immunosorbent assay (ELISA). Data are shown as mean ± standard error of the mean ($n = 9$ for C3H/HeN, BALB/c and C57BL/6; $n = 4$ for DBA/2, B6C3F1 and BDF1).

production of C3H/HeN mice was much higher than that of other strains (Fig. 2b). These observations lead us to speculate that IL-4 and IFN-γ produced by NKT cells work as promoting and suppressing factors, respectively, during NKT cell proliferation.

NKT cell proliferation partially depends on IL-4 and is enhanced by Th2 cytokines

We next examined the influence of IL-4 on NKT cell proliferation *in vitro*. Proliferation of these cells was accelerated by addition of IL-4 at the start of the culture period, an effect that could be partially suppressed by neutralization of IL-4 (Fig. 3). In the C3H/HeN strain, where proliferation of NKT cells was not robust, a more significant induction of proliferation by IL-4 was observed (Fig. 4). In addition, neutralization of IFN-γ using antibodies did not significantly change the proportion of NKT cells in the total cell population. However, this did appear to up-regulate the total number of living cells and lead to a concomitant increase in the total number of NKT cells (Fig. 4b). Only NKT cells can produce IL-4 when cultured with α-GalCer and IL-2,[23] so IL-4 must act as an autocrine growth factor in the expansion of NKT cells in this context.

The proportion of intracellular IFN-γ high positive NKT cells is reduced by addition of IL-4

Exogenous IL-4 promoted NKT cell expansion in C3H/HeN mice, as shown in Figs 3 and 4. We next examined

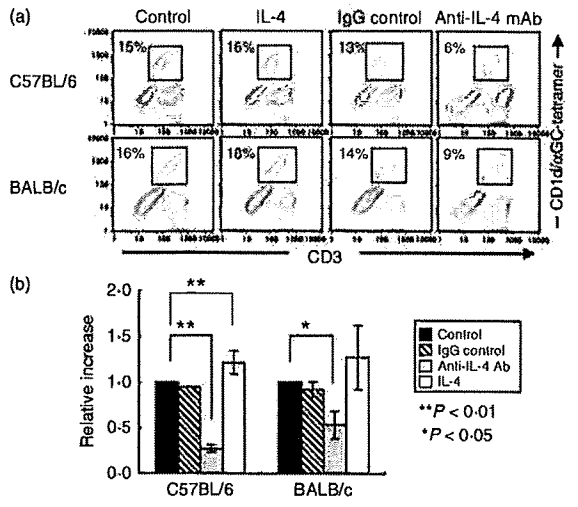

Figure 3. Expansion of natural killer T (NKT) cells in the presence or absence of interleukin (IL)-4. (a) Spleen cells (1×10^6 cells/ml) were cultured with 50 ng/ml α-galactosylceramide (α-GalCer) and 100 U/ml IL-2 for 4 days with IL-4 (10 ng/ml) or anti-IL-4 monoclonal antibody (mAb) (1 mg/ml). The percentages of NKT cells are shown. Data are representative of replicate experiments. (b) The relative increase was based on absolute numbers of NKT cells and was compared with control expansion culture. Data are shown as mean ± standard deviation for five independent experiments. A paired two-tailed Student's *t*-test was used for statistical analysis (*$P < 0·05$; **$P < 0·01$).

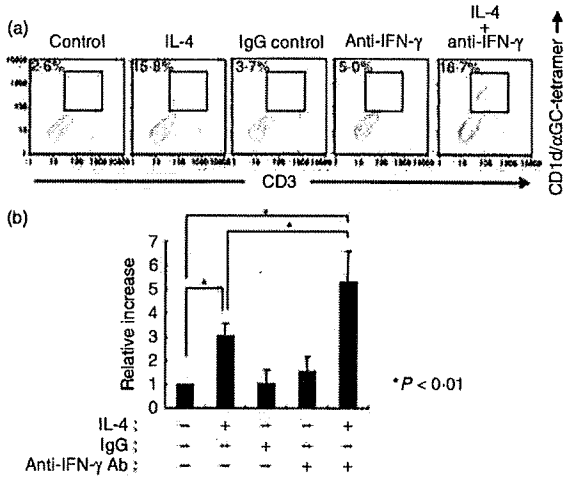

Figure 4. Expansion of natural killer T (NKT) cells from C3H/HeN strain mice in conditions that favour production of T helper type 2 (Th2)-biased cytokines. (a) Spleen cells (1×10^6 cells/ml) were cultured with 50 ng/ml α-galactosylceramide (α-GalCer) and 100 U/ml interleukin (IL)-2 and with IL-4 (10 ng/ml) and/or anti-interferon (IFN)-γ monoclonal antibody (mAb) (1 mg/ml) for 4 days. The percentages of NKT cells are shown. Data are representative of replicate experiments. (b) The relative increase was based on absolute numbers of NKT cells and was compared with the control expansion culture. Data are shown as mean ± standard deviation for seven independent experiments. A paired two-tailed Student's *t*-test was used for statistical analysis (*$P < 0·01$).

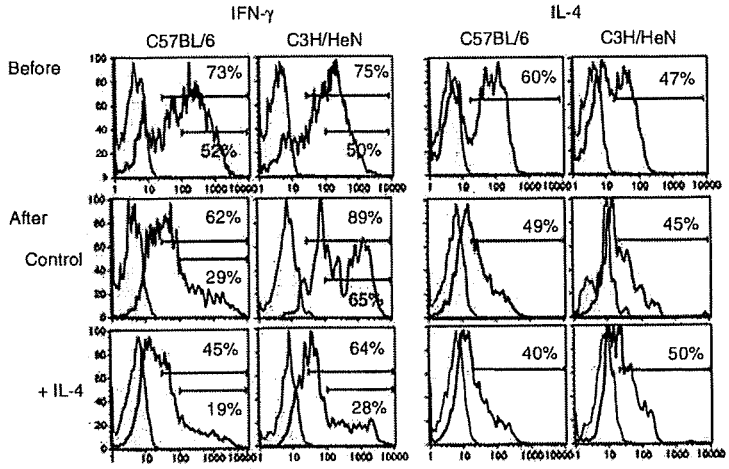

Figure 5. Cytokine production profile of natural killer T (NKT) cells treated with interleukin (IL)-4. Intracellular cytokine staining for interferon (IFN)-γ and IL-4 in NKT cells that were fresh (upper), cultured (middle), or cultured with additional IL-4 (lower) is shown. The cells were stimulated with phorbol 12-myristate 13-acetate (PMA) and ionomycin for 3 hr, stained with anti-CD3 monoclonal antibody (mAb), CD1d/α-galactosylceramide (α-GalCer) tetramer and anti-IFN-γ, anti-IL-4, or an isotype control mAb, and then detected and sorted via flow cytometry. Histogram panels for CD1d/α-GalCer-tetramer$^+$ CD3$^+$ cells are shown. Closed histograms indicate isotype controls. The percentage of total positive and high positive cells are indicated in the histograms. Data are representative of replicate experiments.

whether NKT cells cultured in Th2 conditions produced IFN-γ and IL-4. After 4 days of culture with α-GalCer and IL-2, intracellular IFN-γ- and IL-4-positive NKT cells were observed in both strains of mice. However, the proportion of intracellular IFN-γ high positive NKT cells was reduced when the cells were cultured with additional IL-4 (Fig. 5). In contrast to IFN-γ, the proportion of IL-4-positive NKT cells did not differ between cultures with and without IL-4. Therefore, NKT cells expanding as a result of induction with additional IL-4 displayed a polarized Th2 phenotype.

NKT cell expansion is accelerated by Th2-biased cytokine conditions

The SJL/J mouse strain is defective in cytokine production by NKT cells, as a consequence of a loss of high-affinity TCR to CD1d, which results from a deletion of the TCR Vβ8 subfamily genomic loci.[28,29] The proportion of NKT cells in the spleens of these mice was lower than that observed for other strains (Fig. 6a), and IFN-γ and IL-4 production after α-GalCer stimulation was also lower than that observed for other strains tested in this study (data not shown). NKT cells from SJL/J mice proliferated even in the absence of additional IL-4, as was observed for NKT cells from C57BL/6 mice. Moreover, similar to findings for NKT cells from C3H/HeN mice, the NKT cell proliferation effect could be enhanced by addition of IL-4 and further enhanced by addition of IL-4 combined with neutralization of IFN-γ (Fig. 6b).

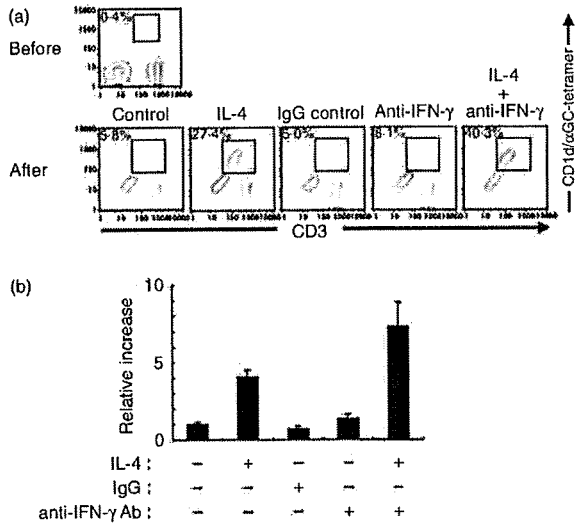

Figure 6. Expansion of natural killer T (NKT) cells from SJL/J mice *in vitro*. (a) Spleen cells (1×10^6 cells/ml) were cultured with 50 ng/ml α-galactosylceramide (α-GalCer) and 100 U/ml interleukin (IL)-2 for 4 days with IL-4 (10 ng/ml) and/or anti-interferon (IFN)-γ monoclonal antibody (mAb) (1 mg/ml). The percentages of NKT cells are shown. Data are representative of replicate experiments. (b) The relative increase was based on absolute numbers of NKT cells and was compared with the control expansion culture. Data are shown as the mean of three wells ± standard deviation. Similar results were obtained in two independent experiments.

Discussion

In a previous study in which we induced expansion of NKT cells collected from human peripheral blood, we

observed wide variation in the efficiency of NKT cell expansion.[21] Similarly, when mouse NKT cells were induced to proliferate using similar methods in the present study, the ratios of expanding cell types were distinctly different in cells obtained from different mouse strains (Fig. 1). This suggests that genetic background influences or controls the difference in proliferation efficiency observed in humans and mice. However, we could not rule out the alternative possibility that the effect was a result of bipolar expansion of the cells, rather than originating from genetic variation in one or a few loci.

In this study, we have shown that the amount of IL-4 in the culture supernatant was related to the efficiency of NKT cell expansion induced by α-GalCer and IL-2. Previous studies revealed that addition of exogenous IL-2, IL-7 and IL-15 was able to augment NKT cell expansion by α-GalCer.[30–34] Similarly, in the present study we found that exogenous IL-2 augmented α-GalCer-induced NKT cell expansion in various mouse strains, with the exception of C3H/HeN mice. Moreover, addition of exogenous IL-4 promoted α-GalCer-induced NKT cell expansion in spleen cells from C3H/HeN mice. It has been shown that only NKT cells have the ability to produce IL-4 in this culture.[23] IL-4 might therefore be an autocrine or paracrine growth factor in α-GalCer-induced NKT cell expansion.

NKT cells, NK cells and some T cells when cultured with α-GalCer and IL-2 produce IFN-γ.[23] In contrast to IL-4, the amount of IFN-γ did not correlate with the efficiency of NKT cell expansion. Furthermore, we found that NKT cell proliferation in C3H/HeN mice was slightly increased by neutralization of IFN-γ in the culture. These results suggest that IFN-γ partially inhibits NKT cell expansion by α-GalCer. Interestingly, we found an inverse correlation between the IFN-γ:IL-4 ratio in the culture supernatant after 24 hr of culture and the efficiency of NKT cell proliferation (data not shown). Although higher amounts of IL-4 were detected in the culture of cells from C3H/HeN mice than in the culture of cells from C57BL/6 mice after 24 hr of culture, α-GalCer stimulated spleen cells from C3H/Ne mice produced higher amounts of IFN-γ and exhibited the highest IFN-γ:IL-4 ratio of all mouse strains tested. These results may explain the failure of NKT cell expansion in spleen cells from C3H/HeN mice.

The balance between the production of IFN-γ and the production of IL-4 by NKT cells is influenced by microenvironmental factors such as cytokines and antigen-presenting cells.[20,35–38] IL-7 and IL-12 selectively enhance IL-4 production by NKT cells.[35,36] Antigen-presenting cells such as α-GalCer-pulsed B cells selectively elicit weak IL-4 but not IFN-γ production from NKT cells.[37] There is a high IFN-γ:IL-4 ratio in cultures of spleen cells from C3H/HeN mice, which is caused by splenic NKT cells (A. Iizuka *et al.*, unpublished data) Moreover, it has been reported that the balance of IFN-γ:IL-4 production by NKT cells is developmentally controlled.[39,40] At immature stages, NKT cells predominantly produce IL-4, whereas IFN-γ secretion increases during the course of development.[39] Moreover, immature NKT cells have the ability to proliferate as compared with mature NKT cells.[39] Therefore, NKT cells in the spleen of C3H/HeN mice may be more mature than those of C57BL/6 mice, or contain only a few immature NKT cells. We assume that the failure of proliferation and the high IFN-γ:IL-4 cytokine production ratio of NKT cells in the spleen of C3H/HeN mice were attributable to their maturation stage.

Although IL-4 has opposite effects to IFN-γ and suppresses the Th1 immune response, IL-4 induces proliferation of human IL-13$^+$ NK cells[41] and CD8$^+$ T cells.[42] We found that Th2 culture conditions (in the presence of IL-4 and anti-IFN-γ mAb) facilitated NKT cell expansion induced by α-GalCer and IL-2 even in C3H/HeN and SJL/J mice. IL-4 also induces IFN-γ production by NK and NKT cells *in vivo*.[43] However, the proportion of IFN-γ-positive, but not IL-4-positive, NKT cells decreased when cells were cultured in the presence of IL-4. As in human immature IL-13$^+$ NK cells,[41] IL-4 may induce expansion of developmentally immature NKT cells which have a Th2-biased phenotype.

NKT cell maturation is controlled by the transcription factor T-bet.[44,45] Terminally differentiated NKT cells acquire a strong ability to produce IFN-γ and elicit cytotoxicity.[44] Assuming that expanded Th2-biased NKT cells after culture with α-GalCer, IL-2 and IL-4 are immature cells, it will be possible to induce terminally differentiated Th1-biased NKT cells for Th1 cell immunotherapy, such as cancer cell therapy.

Acknowledgements

We thank the Pharmaceutical Research Laboratory, Kirin Brewery Co., Ltd (Gunma, Japan) for providing α-GalCer. This work was supported in part by a grant-in-aid for the Third-Term Comprehensive 10-Year Strategy for Cancer Control and for Cancer Research from the Ministry of Health, Labour and Welfare of Japan.

References

1 Ballas ZK, Rasmussen W. NK1.1$^+$ thymocytes. Adult murine CD4$^-$, CD8$^-$ thymocytes contain an NK1.1$^+$, CD3$^+$, CD5^{hi}, CD44^{hi}, TCR-Vβ 8$^+$ subset. *J Immunol* 1990; 145:1039–45.

2 Godfrey DI, Hammond KJ, Poulton LD, Smyth MJ, Baxter AG. NKT cells: facts, functions and fallacies. *Immunol Today* 2000; 21:573–83.

3 Makino Y, Koseki H, Adachi Y, Akasaka T, Tsuchida K, Taniguchi M. Extrathymic differentiation of a T cell bearing invariant Vα14 Jα281 TCR. *Int Rev Immunol* 1994; 11:31–46.

4 Gapin L, Matsuda JL, Surh CD, Kronenberg M. NKT cells derive from double-positive thymocytes that are positively selected by CD1d. *Nat Immunol* 2001; 2:971–8.

5 Mattner J, Debord KL, Ismail N *et al.* Exogenous and endogenous glycolipid antigens activate NKT cells during microbial infections. *Nature* 2005; **434**:525–9.

6 Nishimura T, Santa K, Yahata T *et al.* Involvement of IL-4-producing Vβ 8.2^{+} CD4^{+} CD62L^{-} CD45RB^{-} T cells in non-MHC gene-controlled predisposition toward skewing into T helper type-2 immunity in BALB/c mice. *J Immunol* 1997; **158**:5698–706.

7 van Der Vliet HJ, Nishi N, de Gruijl TD, von Blomberg BM, van den Eertwegh AJ, Pinedo HM, Giaccone G, Scheper RJ. Human natural killer T cells acquire a memory-activated phenotype before birth. *Blood* 2000; **95**:2440–2.

8 Godfrey DI, Kronenberg M. Going both ways: immune regulation via CD1d-dependent NKT cells. *J Clin Invest* 2004; **114**:1379–88.

9 Arase H, Arase N, Kobayashi Y, Nishimura Y, Yonehara S, Onoe K. Cytotoxicity of fresh NK1.1^{+} T cell receptor α/β^{+} thymocytes against a CD4^{+}8^{+} thymocyte population associated with intact Fas antigen expression on the target. *J Exp Med* 1994; **180**:423–32.

10 Nieda M, Nicol A, Koezuka Y *et al.* TRAIL expression by activated human CD4^{+}Vα24NKT cells induces in vitro and in vivo apoptosis of human acute myeloid leukemia cells. *Blood* 2001; **97**:2067–74.

11 Nicol A, Nieda M, Koezuka Y, Porcelli S, Suzuki K, Tadokoro K, Durrant S, Juji T. Human invariant Vα24^{+} natural killer T cells activated by α-galactosylceramide (KRN7000) have cytotoxic anti-tumour activity through mechanisms distinct from T cells and natural killer cells. *Immunology* 2000; **99**:229–34.

12 Mattarollo SR, Kenna T, Nieda M, Nicol AJ. Chemotherapy pretreatment sensitizes solid tumor-derived cell lines to Vα24^{+} NKT cell-mediated cytotoxicity. *Int J Cancer* 2006; **119**:630–7.

13 Smyth MJ, Thia KY, Street SE *et al.* Differential tumor surveillance by natural killer (NK) and NKT cells. *J Exp Med* 2000; **191**:661–8.

14 Seino K, Motohashi S, Fujisawa T, Nakayama T, Taniguchi M. Natural killer T cell-mediated antitumor immune responses and their clinical applications. *Cancer Sci* 2006; **97**:807–12.

15 Metelitsa LS, Naidenko OV, Kant A, Wu HW, Loza MJ, Perussia B, Kronenberg M, Seeger RC. Human NKT cells mediate antitumor cytotoxicity directly by recognizing target cell CD1d with bound ligand or indirectly by producing IL-2 to activate NK cells. *J Immunol* 2001; **167**:3114–22.

16 Giaccone G, Punt CJ, Ando Y *et al.* A phase I study of the natural killer T-cell ligand α-galactosylceramide (KRN7000) in patients with solid tumors. *Clin Cancer Res* 2002; **8**:3702–9.

17 Shimizu K, Hidaka M, Kadowaki N *et al.* Evaluation of the function of human invariant NKT cells from cancer patients using alpha-galactosylceramide-loaded murine dendritic cells. *J Immunol* 2006; **177**:3484–92.

18 Parekh VV, Wilson MT, Olivares-Villagomez D, Singh AK, Wu L, Wang CR, Joyce S, Van Kaer L. Glycolipid antigen induces long-term natural killer T cell anergy in mice. *J Clin Invest* 2005; **115**:2572–83.

19 Ishikawa A, Motohashi S, Ishikawa E *et al.* A phase I study of α-galactosylceramide (KRN7000)-pulsed dendritic cells in patients with advanced and recurrent non-small cell lung cancer. *Clin Cancer Res* 2005; **11**:1910–7.

20 van der Vliet HJ, Molling JW, Nishi N *et al.* Polarization of Vα24^{+} Vβ11^{+} natural killer T cells of healthy volunteers and cancer patients using α-galactosylceramide-loaded and environmentally instructed dendritic cells. *Cancer Res* 2003; **63**:4101–6.

21 Harada Y, Imataki O, Heike Y *et al.* Expansion of α-galactosylceramide-stimulated Vα24^{+} NKT cells cultured in the absence of animal materials. *J Immunother* 2005; **28**:314–21.

22 Kadowaki N, Antonenko S, Ho S, Rissoan MC, Soumelis V, Porcelli SA, Lanier LL, Liu YJ. Distinct cytokine profiles of neonatal natural killer T cells after expansion with subsets of dendritic cells. *J Exp Med* 2001; **193**:1221–6.

23 Ikarashi Y, Iizuka A, Heike Y, Yoshida M, Takaue Y, Wakasugi H. Cytokine production and migration of in vitro-expanded NK1.1^{-} invariant Vα14 natural killer T (Vα14i NKT) cells using α-galactosylceramide and IL-2. *Immunol Lett* 2005; **101**:160–7.

24 Matsuda JL, Naidenko OV, Gapin L, Nakayama T, Taniguchi M, Wang CR, Koezuka Y, Kronenberg M. Tracking the response of natural killer T cells to a glycolipid antigen using CD1d tetramers. *J Exp Med* 2000; **192**:741–54.

25 Smyth MJ, Crowe NY, Pellicci DG, Kyparissoudis K, Kelly JM, Takeda K, Yagita H, Godfrey DI. Sequential production of interferon-gamma by NK1.1^{+} T cells and natural killer cells is essential for the antimetastatic effect of α-galactosylceramide. *Blood* 2002; **99**:1259–66.

26 Kambayashi T, Assarsson E, Lukacher AE, Ljunggren HG, Jensen PE. Memory CD8^{+} T cells provide an early source of IFN-γ. *J Immunol* 2003; **170**:2399–408.

27 Eberl G, MacDonald HR. Rapid death and regeneration of NKT cells in anti-CD3ε- or IL-12-treated mice: a major role for bone marrow in NKT cell homeostasis. *Immunity* 1998; **9**:345–53.

28 Serizawa I, Koezuka Y, Amao H, Saito TR, Takahashi KW. Functional natural killer T cells in experimental mouse strains, including NK1.1^{-} strains. *Exp Anim* 2000; **49**:171–80.

29 Beutner U, Launois P, Ohteki T, Louis JA, MacDonald HR. Natural killer-like T cells develop in SJL mice despite genetically distinct defects in NK1.1 expression and in inducible interleukin-4 production. *Eur J Immunol* 1997; **27**:928–34.

30 Asada-Mikami R, Heike Y, Harada Y *et al.* Increased expansion of Vα24^{+} T cells derived from G-CSF-mobilized peripheral blood stem cells as compared to peripheral blood mononuclear cells following α-galactosylceramide stimulation. *Cancer Sci* 2003; **94**:383–8.

31 Imataki O, Heike Y, Ishida T, Takaue Y, Ikarashi Y, Yoshida M, Wakasugi H, Kakizoe T. Efficient ex vivo expansion of Vα24^{+} NKT cells derived from G-CSF-mobilized blood cells. *J Immunother* 2006; **29**:320–7.

32 Brossay L, Chioda M, Burdin N, Koezuka Y, Casorati G, Dellabona P, Kronenberg M. CD1d-mediated recognition of an α-galactosylceramide by natural killer T cells is highly conserved through mammalian evolution. *J Exp Med* 1998; **188**:1521–8.

33 Nishi N, van der Vliet HJ, Koezuka Y, von Blomberg BM, Scheper RJ, Pinedo HM, Giaccone G. Synergistic effect of KRN7000 with interleukin-15, -7, and -2 on the expansion of human Vα 24^{+}V β11^{+} T cells *in vitro*. *Hum Immunol* 2000; **60**:357–65.

34 van der Vliet HJ, Nishi N, Koezuka Y *et al.* Potent expansion of human natural killer T cells using α-galactosylceramide

(KRN7000)-loaded monocyte-derived dendritic cells, cultured in the presence of IL-7 and IL-15. *J Immunol Meth* 2001; 247:61–72.

35 Hameg A, Gouarin C, Gombert JM, Hong S, Van Kaer L, Bach JF, Herbelin A. IL-7 up-regulates IL-4 production by splenic NK1.1$^+$ and NK1.1$^-$ MHC class I-like/CD1-dependent CD4$^+$ T cells. *J Immunol* 1999; 162:7067–74.

36 Zhu R, Diem S, Araujo LM *et al.* The Pro-Th1 cytokine IL-12 enhances IL-4 production by invariant NKT cells: relevance for T cell-mediated hepatitis. *J Immunol* 2007; 178:5435–42.

37 Bezbradica JS, Stanic AK, Matsuki N *et al.* Distinct roles of dendritic cells and B cells in Va14Ja18 natural T cell activation in vivo. *J Immunol* 2005; 174:4696–705.

38 Minami K, Yanagawa Y, Iwabuchi K, Shinohara N, Harabayashi T, Nonomura K, Onoe K. Negative feedback regulation of T helper type 1 (Th1)/Th2 cytokine balance via dendritic cell and natural killer T cell interactions. *Blood* 2005; 106:1685–93.

39 Benlagha K, Kyin T, Beavis A, Teyton L, Bendelac A. A thymic precursor to the NK T cell lineage. *Science* 2002; 296:553–5.

40 Pellicci DG, Hammond KJ, Uldrich AP, Baxter AG, Smyth MJ, Godfrey DI. A natural killer T (NKT) cell developmental pathway involving a thymus-dependent NK1.1$^-$CD4$^+$ CD1d-dependent precursor stage. *J Exp Med* 2002; 195:835–44.

41 Lora MJ, Perussia B. Final steps of natural killer cell maturation: a model for type 1-type 2 differentiation? *Nat Immunol* 2001; 2:917–24.

42 Ueda N, Kuki H, Kaminura D *et al.* CD1d-restricted NKT cell activation enhanced homeostatic proliferation of CD8$^+$ T cells in a manner dependent on IL-4. *Int Immunol* 2006; 18:1397–404.

43 Morris SC, Orekhova T, Meadows MJ, Heidorn SM, Yang J, Finkelman FD. IL-4 induces in vivo production of IFN-γ by NK and NKT cells. *J Immunol* 2006; 176:5299–305.

44 Townsend MJ, Weinmann AS, Matsuda JL, Salomon R, Farnham PJ, Biron CA, Gapin L, Glimcher LH. T-bet regulates the terminal maturation and homeostasis of NK and Vα14i NKT cells. *Immunity* 2004; 20:477–94.

45 Matsuda JL, Zhang Q, Ndonye R, Richardson SK, Howell AR, Gapin L. T-bet concomitantly controls migration, survival, and effector functions during the development of Vα14i NKT cells. *Blood* 2006; 107:2797–805.

A Novel Antiangiogenic Effect for Telomerase-Specific Virotherapy through Host Immune System[1]

Yoshihiro Ikeda,* Toru Kojima,* Shinji Kuroda,* Yoshikatsu Endo,* Ryo Sakai,* Masayoshi Hioki,* Hiroyuki Kishimoto,* Futoshi Uno,* Shunsuke Kagawa,*† Yuichi Watanabe,‡ Yuuri Hashimoto,‡ Yasuo Urata,‡ Noriaki Tanaka,* and Toshiyoshi Fujiwara[2]*†

Soluble factors in the tumor microenvironment may influence the process of angiogenesis; a process essential for the growth and progression of malignant tumors. In this study, we describe a novel antiangiogenic effect of conditional replication-selective adenovirus through the stimulation of host immune reaction. An attenuated adenovirus (OBP-301, Telomelysin), in which the human telomerase reverse transcriptase promoter element drives expression of E1 genes, could replicate in and cause selective lysis of cancer cells. Mixed lymphocyte-tumor cell culture demonstrated that OBP-301-infected cancer cells stimulated PBMC to produce IFN-γ into the supernatants. When the supernatants were subjected to the assay of in vitro angiogenesis, the tube formation of HUVECs was inhibited more efficiently than recombinant IFN-γ. Moreover, in vivo angiogenic assay using a membrane-diffusion chamber system s.c. transplanted in *nu/nu* mice showed that tumor cell-induced neovascularization was markedly reduced when the chambers contained the mixed lymphocyte-tumor cell culture supernatants. The growth of s.c. murine colon tumors in syngenic mice was significantly inhibited due to the reduced vascularity by intratumoral injection of OBP-301. The antitumor as well as antiangiogenic effects, however, were less apparent in SCID mice due to the lack of host immune responses. Our data suggest that OBP-301 seems to have antiangiogenic properties through the stimulation of host immune cells to produce endogenous antiangiogenic factors such as IFN-γ. *The Journal of Immunology,* 2009, 182: 1763–1769.

Angiogenesis is the development of new capillaries from preexisting capillary blood vessels and is necessary for the growth of solid tumors beyond 1–2 mm in diameter (1). Targeting the angiogenic process is therefore regarded as a promising strategy in cancer therapy. Angiogenesis consists of dissolution of the basement membrane, migration and proliferation of endothelial cells, canalization, branching and formation of vascular loops, and formation of a basement membrane (2). These steps might be regulated by the local balance between the amount of angiogenic stimulators and inhibitors (3–5). As cells undergo malignant transformation, angiogenic mitogens such as vascular endothelial growth factor (VEGF),[3] basic fibroblast growth factor, platelet-derived epithelial cell growth factor, and TGF become dominant, causing the aberrant angiogenesis. In contrast, many endogenous angiogenic inhibitors such as platelet factor 4, thrombospondin 1, angiostatin, endostatin, various antiangiogenic peptides, hormone metabolites, and cytokines constitutively suppress angiogenesis in normal tissues (6). These scenarios suggest the possibility that endogenous angiogenic inhibitors that outweigh the stimulators could turn off the angiogenic switch.

Recent studies have demonstrated that the tumor microenvironment, which orchestrates with the host immune system, is a critical component of both tumor progression and tumor suppression (7). Indeed, the production of cytokines at tumor sites can either stimulate or inhibit tumor growth and progression (8). These findings provide a unique therapeutic opportunity based on selective and locoregional production of endogenous antitumor mediators such as angiogenic inhibitors. We reported previously that telomerase-specific replication-competent adenovirus (Telomelysin, OBP-301), in which the human telomerase reverse transcriptase promoter element drives the expression of *E1A* and *E1B* genes linked with an internal ribosomal entry sequence, induced selective E1 expression and efficiently killed human cancer cells, but not normal human fibroblasts (9–12). Although the precise molecular mechanism of OBP-301-induced cell death is still unclear, the process of oncolysis is morphologically distinct from apoptosis and necrosis. We found that tumor cells killed by OBP-301 infection could stimulate host immune cells more efficiently compared with chemotherapeutic drug-induced apoptotic cells and necrotic cells by freeze/thaw, thus enhancing the antitumor immune response (13). These results suggest that oncolytic virus is effective not only as a direct cytotoxic drug but also as an immunostimulatory agent that could modify the tumor microenvironment.

In the present article, we explored whether OBP-301-infected oncolytic cells can activate host immune cells and influence tumor

*Division of Surgical Oncology, Department of Surgery, Okayama University Graduate School of Medicine, Dentistry and Pharmaceutical Sciences, Okayama, †Center for Gene and Cell Therapy, Okayama University Hospital, Okayama, and ‡Oncolys BioPharma, Tokyo, Japan

Received for publication July 22, 2008. Accepted for publication November 26, 2008.

The costs of publication of this article were defrayed in part by the payment of page charges. This article must therefore be hereby marked *advertisement* in accordance with 18 U.S.C. Section 1734 solely to indicate this fact.

[1] This work was supported by Grants-in-Aid from the Ministry of Education, Science, and Culture, Japan (to T.F.) and grants from the Ministry of Health and Welfare, Japan (to T.F.).

[2] Address correspondence and reprint requests to Dr. Toshiyoshi Fujiwara, Center for Gene and Cell Therapy, Okayama University Hospital, 2-5-1 Shikata-cho, Okayama 700-8558, Japan. E-mail address: toshi_f@md.okayama-u.ac.jp

[3] Abbreviations used in this paper: VEGF, vascular endothelial growth factor; MLTC, mixed lymphocyte-tumor cell culture; MOI, multiplicity of infection.

cell-mediated angiogenesis in vitro and in vivo. Antineoplastic effect of intratumoral administration of OBP-301 on s.c. murine colon tumors transplanted was compared in syngenic immunocompetent mice and SCID mice. Finally, we examined the effect of neutralizing anti-IFN-γ Ab on OBP-301-mediated antiangiogenic potential in vivo.

Materials and Methods

Cell lines and reagents

The human colorectal carcinoma cell lines SW620 (HLA-A02/A24) and the murine colon adenocarcinoma cell line Colon-26 were maintained in vitro in RPMI 1640 supplemented with 10% FCS, 100 U/ml penicillin, and 100 mg/ml streptomycin. Recombinant human IFN-γ was purchased from Peprotech.

Mice

Female BALB/c (BALB/cAnNCrlCrlj), BALB/c *nu/nu* (CAnN.Cg-*Foxn1*^{nu}/CrlCrlj), and SCID (CB17/Icr-*Prkdc*^{scid}/CrlCrlj) mice, 5–6 wk of age, were purchased from Charles River Japan Breeding Laboratories. Animals were housed under specific pathogen-free conditions in accordance with the guidelines of the Institutional Animal Care and Use Committee.

Adenovirus

The recombinant replication-selective, tumor-specific adenovirus vector OBP-301 (Telomelysin), in which the human telomerase reverse transcriptase promoter element drives the expression of *E1A* and *E1B* genes linked with an internal ribosomal entry sequence, was constructed and previously characterized (9–12). The virus was purified by $CsCl_2$ step gradient ultracentrifugation followed by $CsCl_2$ linear gradient ultracentrifugation.

Cell viability assay

XTT assay was performed to measure cell viability. Briefly, cells were plated on 96-well plates at 5×10^3 per well 24 h before treatment and then infected with OBP-301. Cell viability was determined at the times indicated by using a Cell Proliferation kit II (Roche Molecular Biochemicals) according to the protocol provided by the manufacturer.

Mixed lymphocyte-tumor cell culture (MLTC) and cytokine production assay

For MLTC, SW620 tumor cells were infected with OBP-301 at a multiplicity of infection (MOI) of 10, washed three times in PBS 72 h after infection, and then cocultured with PBMC at a ratio of 1:40. The supernatant was collected at the indicated times and stored at −80°C until assay. The concentration of IFN-γ was measured with ELISA kits (BioSource International).

In vitro angiogenesis assay

In vitro angiogenesis was assessed based on the formation of capillary-like structures by HUVECs cocultured with human diploid fibroblasts according to the instructions provided with the angiogenesis kit (Kurabo). In brief, the HUVECs were incubated in a medium containing the diluted supernatants of MLTC or recombinant IFN-γ in the presence or absence of VEGF (10 ng/ml). The medium was replaced at days 4, 7, and 9. At day 11, the HUVECs were fixed and stained by using an anti-human CD31 Ab (Kurabo) according to the instructions provided. The formation of the capillary network was observed with a microscope at a magnification of ×40.

In vivo assay for tumor angiogenesis

In vivo angiogenesis was determined using the dorsal air-sac method (14). Briefly, 2×10^6 SW620 cells were suspended in PBS containing the diluted supernatants of MLTC or control medium, and placed into round-shaped chambers that consisted of a ring covered with cellulose ester filters (pore size, 0.45 μm; Millipore) on both sides. These chambers were implanted into a dorsal air sac produced in female BALB/c *nu/nu* mice by the injection of 10 ml of air. Five mice in each group were sacrificed on day 5, and the formation of a dense capillary network in s.c. regions was examined under a dissecting microscope. The neovascularization was assessed semiquantitatively by counting the number of cork screw vessels. For each slide, a total of three fields at a magnification of ×4 were selected at random, and the scores were averaged.

In vivo tumor growth and determination of microvessels

Female BALB/c and SCID mice were s.c. implanted with 2×10^6 Colon-26 cells. When tumors grew to ~5–6 mm in diameter, the mice were randomly assigned into three groups and a 100 μl of solution containing 1×10^8 PFU of dl312 or OBP-301, or PBS was injected into the tumor on days 1, 3, and 5. Tumors were measured for perpendicular diameters every 3 or 4 days, and tumor volume (in cubic millimeters) was calculated using the following formula: $a \times b^2 \times 0.5$, where a is the longest diameter, b is the shortest diameter, and 0.5 is a constant to calculate the volume of an ellipsoid. For histological analysis, 2 wk after treatment, the tumors were harvested, embedded in Tissue Tek (Sakura), cut into 5 μm-thick sections, and assessed by a standard H&E and immunohistochemical staining using a rat anti-mouse mAb against CD31 (BD Pharmingen). The experimental protocol was approved by the Ethics Review Committee for Animal Experimentation of Okayama University Graduate School of Medicine, Dentistry, and Pharmaceutical Sciences.

In vivo inhibition of IFN-γ with neutralizing Abs

For neutralizing IFN-γ, mice were i.p. administered 200 μg of rat anti-mouse IFN-γ mAb (XMG1.2; BD Pharmingen) 1 day before the first injection of OBP-301 and on days 1 and 3 after the first injection. Control mice received i.p. administration of isotype-matched rat IgG1 (BD Pharmingen).

Statistical analysis

Determination of significant differences among groups was assessed by calculating the value of Student's t test using the original data analysis. Statistical significance was defined at $p < 0.01$.

Results

Effect of OBP-301-infected human colorectal cancer cells on PBMC in vitro

First, we examined whether OBP-301 infection affects the viability of human colorectal cancer cells using the XTT assay. SW620 cells were either mock-infected with culture medium or infected with OBP-301 at an MOI of 1 or 10. As shown in Fig. 1*A*, OBP-301 infection induced death of SW620 cells in a dose-dependent manner. Next, we examined the ability of OBP-301-infected oncolytic cells to stimulate PBMC in MLTC. For this purpose, SW620 cells (HLA-A02/A24) treated with 10 MOI of OBP-301 for 72 h were cocultured with HLA-matched PBMC obtained from HLA-A24$^+$ healthy volunteers at a ratio of 1:40. The production of IFN-γ in the supernatants was then explored by ELISA analysis at the indicated time points. PBMC incubated with OBP-301-infected oncolytic SW620 cells secreted large amounts of IFN-γ as early as 24 h after MLTC, whereas PBMC alone induced little IFN-γ secretion (Fig. 1*B*). The maximum level of IFN-γ was ~250 pg/ml. We previously confirmed that addition of OBP-301 alone without target tumor cells did not affect the cytokine secretion from PBMC into the supernatant, indicating that infection of OBP-301 itself had no apparent effect on PBMC (13). These results suggest that PBMC stimulated with oncolytic tumor cells preferentially secrete high-level IFN-γ.

Inhibition of in vitro and in vivo angiogenesis by MLTC supernatants with OBP-301-infected human tumor cells

In the next step, we investigated the effects of MLTC supernatants with oncolytic SW620 tumor cells and HLA-matched PBMC on VEGF-induced angiogenesis in vitro. The addition of VEGF enhanced the formation of vascular-like structures of HUVECs, although tubule formation was almost absent without VEGF. This VEGF-induced angiogenesis was completely impaired by the addition of MLTC supernatants even at 1/4 dilution (Fig. 2). In contrast, although MLTC supernatants were confirmed to contain ~250 pg/ml IFN-γ, 10-fold more concentration of recombinant IFN-γ was needed to attenuate the tubule formation close to basal levels. The supernatants of PBMC

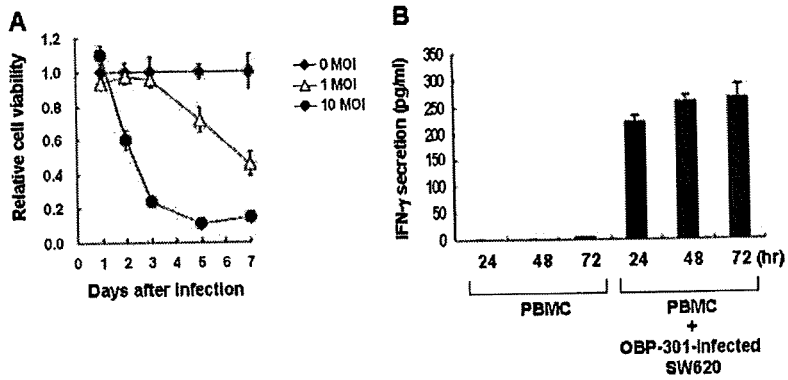

FIGURE 1. In vitro cytopathic effects of OBP-301 and IFN-γ secretion by oncolytic cell-stimulated PBMC. *A*, SW620 human colorectal cancer cells were infected with OBP-301 at indicated MOI values, and surviving cells were quantitated over 7 days by XTT assay. The cell viability of mock-treated cells on day 1 was considered 1.0, and the relative cell viability was calculated. Data are mean ± SD of triplicate experiments. *B*, IFN-γ concentrations in the supernatants of MLTC analyzed by ELISA. SW620 cells were treated with 10 MOI of OBP-301 for 72 h, and then cocultured with PBMCs obtained from HLA-A24$^+$ healthy volunteers for the indicated time periods in MLTC. The culture supernatants were harvested and tested by ELISA for IFN-γ concentrations. As a control, the supernatants of PBMC alone were also examined. Data are mean ± SD of triplicate experiments.

alone had no effect on in vitro angiogenesis. These results suggest that MLTC supernatants may contain more antiangiogenic factors in addition to IFN-γ.

We also assessed whether MLTC supernatants inhibited in vivo angiogenesis induced by human cancer cells. SW620 cells in PBS containing supernatants of OBP-301-infected SW620 cells, PBMC, or both, which were packed into membrane chambers, were implanted into a dorsal air sac produced in *nu/nu* mice. The chambers consisted of membranes that allowed the passage of macromolecules such as IFN-γ, but not cells. Five days after implantation, neovascularization, as demonstrated by the development of capillary networks and curled microvessels in addition to the preexisting vessels, occurred in the dorsal subcutis touched by the chamber, which contained SW620 cells alone. The addition of MLTC supernatants, however, reduced the size and tortuosity of the preexisting vessels, and significantly reduced the development of curled microvessels (Fig. 3). Although the preexisting vessels became thinner by supernatants of OBP-301-infected SW620 cells or PBMC, the number of curled microvessels, which is characteristic of tumor neovasculature, was consistent in these two groups with that in the group compared with SW620 cells alone. Thus, MLTC supernatants exhibited a profound antiangiogenic activity in vivo.

Involvement of host immune activity on antiangiogenic effect of OBP-301

The finding that OBP-301-infected tumor cells stimulated PBMC to produce antiangiogenic factors prompted us to study whether immunodeficiency of host animals could affect the antitumor effect of OBP-301 in vivo. When 2×10^6 Colon-26 murine colon adenocarcinoma cells were inoculated s.c. into BALB/c and SCID mice, palpable tumors appeared in 100% of the mice within 2 wk after tumor injection. Fourteen days after tumor inoculation, animals bearing Colon-26 tumors with a diameter of 5–6 mm were treated with the direct intratumoral injection of 10^8 PFU OBP-301 every 2 days for three cycles. As shown in Fig. 4, treatment with OBP-301 resulted in a significant growth suppression compared with tumors injected with PBS at least for 12 days starting on day 4 after last virus injection ($p < 0.01$) in BALB/c mice; however, OBP-301-mediated antitumor effect was partially impaired in SCID mice, as significant inhibition was observed only for 6 days starting on day 10. Intratumoral injection of replication-deficient dl312 adenovirus had no effect on the tumor growth in BALB/c or SCID mice (data not shown). These results indicate the partial involvement of the host immune system in the OBP-301-mediated antitumor effect.

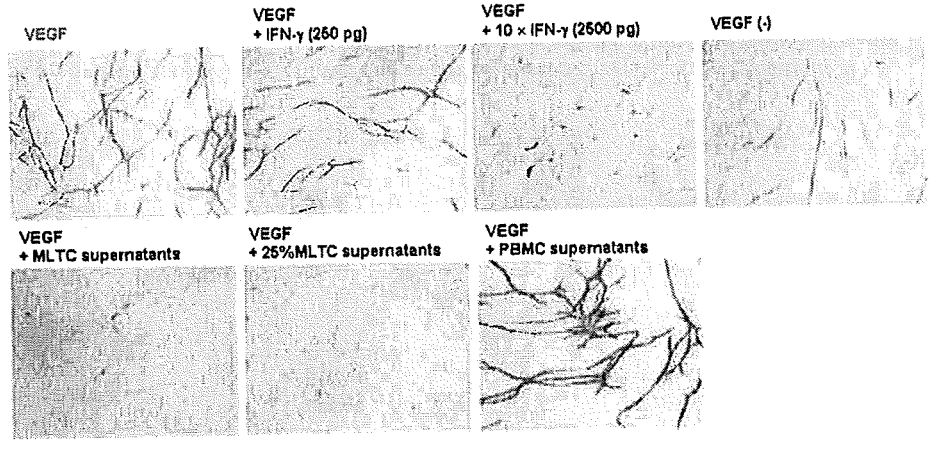

FIGURE 2. Inhibition of in vitro angiogenesis by the supernatants of OBP-301-infected oncolytic cells and PBMC. HUVECs were incubated in a medium containing the supernatants of MLTC obtained 72 h after coculture with OBP-301-infected oncolytic cells and PBMC or recombinant IFN-γ in the presence or absence of VEGF (10 ng/ml). The formation of the capillary network was confirmed by staining with anti-human CD31 Ab on day 11. Representative images depicting formation of capillary-like tube structures by HUVECs are shown. Original magnification is at ×40.

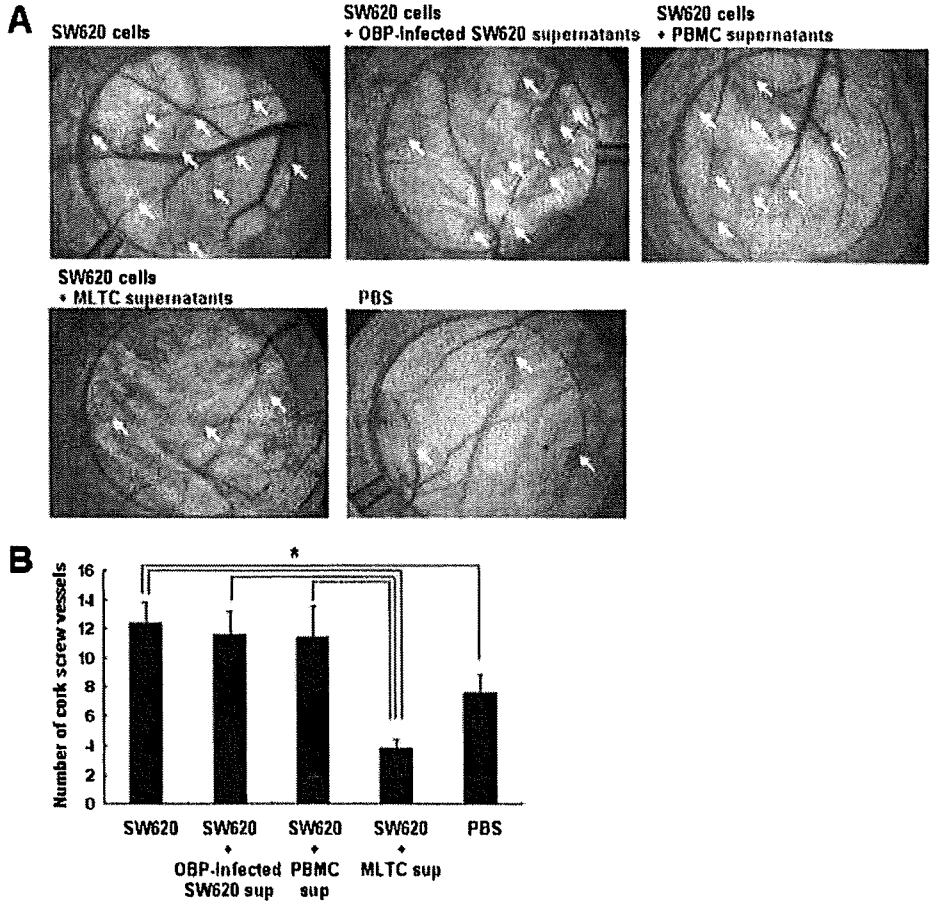

FIGURE 3. Inhibition of tumor cell-mediated in vivo angiogenesis by the supernatants of OBP-301-infected oncolytic cells and PBMC. *A*, SW620 human colorectal tumor cells at a density of 2×10^6 were placed in a diffusion chamber in PBS containing the diluted supernatants of MLTC obtained 72 h after coculture with OBP-301-infected oncolytic cells and PBMC or control mediums, and it was implanted into a dorsal air space produced in BALB/c *nu/nu* mice on day 0. Mice were sacrificed on day 5, and the chamber was removed from the s.c. tissue. A new ring without filters was placed on the same site to mark the position of the chamber. The capillary networks developed inside the rings were photographed to determine the effect of treatments. Representative images of treatment groups are shown. Curled microvessels are shown (arrow). *B*, The number of cork screw vessels was semiquantitatively counted to assess the neovascularization. Data are mean ± SD. *, $p < 0.01$. Similar results were observed in two independent experiments conducted in triplicate.

Antiangiogenic effect of OBP-301 on syngenic and immunodeficient murine tumor models

When Colon-26 s.c. tumors implanted in BALB/c mice were injected with PBS, replication-deficient dl312 adenovirus, or OBP-301. Macroscopically, tumors treated with OBP-301 were consistently smaller than those of the other two cohorts of mice 14 days after last virus injection (Fig. 5*A*). Furthermore, a reddish area was noted on the tumor surface on two of six mice treated with OBP-301, indicating virus-induced intratumoral necrosis of tumor cells in vivo.

To better understand the mechanisms underlying the induction of necrosis following OBP-301 treatment, histologic and immunohistochemical analyses were performed on Colon-26 tumors harvested 14 days after last injection. A standard H&E staining demonstrated the presence of many vessels in tumors injected with PBS or dl312. However, OBP-301-treated tumors showed few vessels. In addition, massive tumor cell death and cellular infiltrates at the central portions of the tumors were observed where OBP-301 was injected (Fig. 5*B*). Immunohistochemical staining of tumor sections with the Ab for CD31 Ag, an endothelial cell marker, also revealed that Colon-26 tumors injected with OBP-301 displayed very few and extremely small blood vessels (Fig. 5*C*). In contrast, OBP-301 injection could not apparently reduce the vessel numbers on Colon-26 tumors implanted in SCID mice (Fig. 5*D*). These in vivo studies demonstrated that inhibition of angiogenesis due to the stimulation of host immune system might be an important mechanism of OBP-301-mediated in vivo antitumor effect.

Contribution of in vivo IFN-γ production to the OBP-301-mediated antiangiogenic effects

Finally, to determine whether IFN-γ is involved in OBP-301-mediated antiangiogenic effects, in vivo neutralizing experiments were performed by using anti-IFN-γ mAb or isotype-matched control mAb. Angiogenesis was reduced by intratumoral injection of

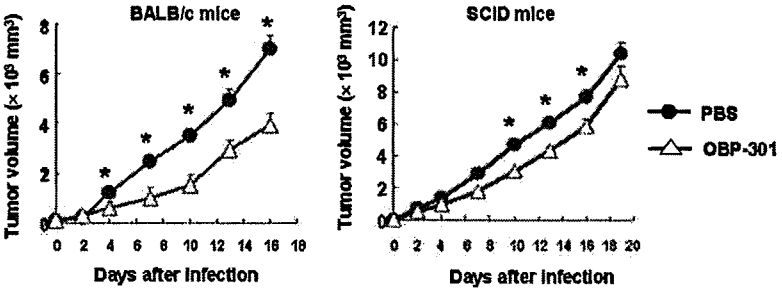

FIGURE 4. Antitumor effects of intratumorally injected OBP-301 against Colon-26 murine colon adenocarcinoma tumors in syngenic immunocompetent BALB/c and immunodeficient SCID mice. Colon-26 cells (2×10^6 cells/each) were injected s.c. into the right flank of mice. OBP-301 (1×10^8 PFU/body) was administered intratumorally for three cycles every 2 days. PBS was used as a control. Six mice were used in each group. Tumor growth was expressed by tumor mean volume ± SD. *, $p < 0.01$.

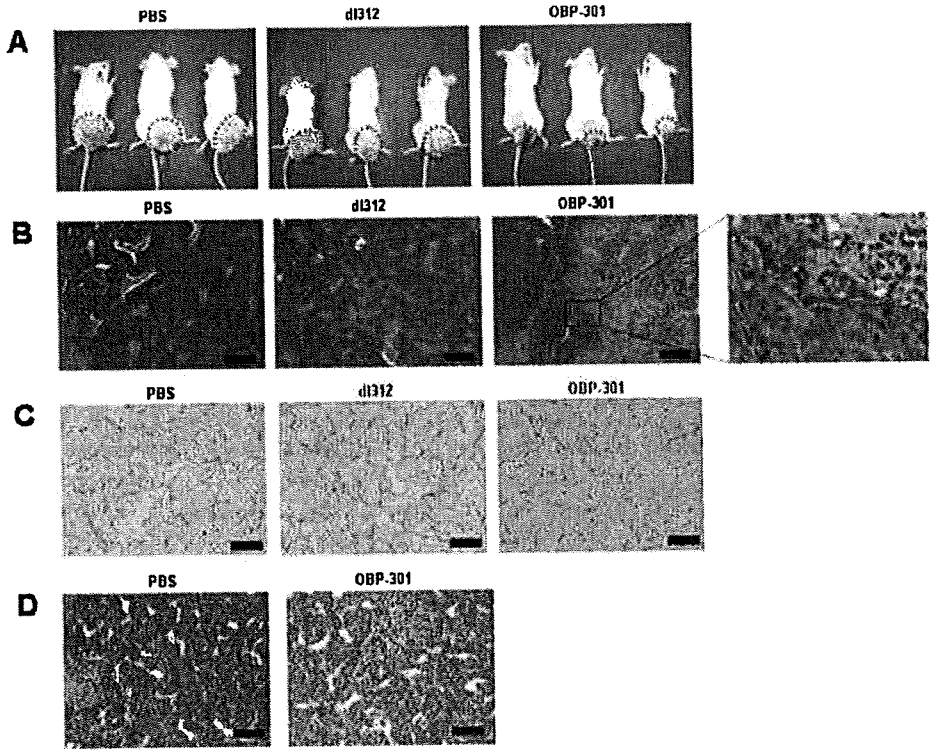

FIGURE 5. Macroscopic and histopathological analysis of Colon-26 tumors treated intratumorally with OBP-301. Colon-26 cells (2×10^6 cells/each) were injected s.c. into the right flank of syngenic BALB/c mice and SCID mice and OBP-301 (1×10^8 PFU/body) was administered intratumorally for three cycles every 2 days as described in Fig. 4. *A*, Macroscopic appearance of Colon-26 tumors on BALB/c mice 14 days after treatment. Note the reddish area on the tumor surface in two mice treated with OBP-301. *B*, Tumor sections were obtained from BALB/c mice 14 days after final administration of OBP-301. Frozen sections of tumors were stained with H&E. Scale bar represents 100 μm, and magnification is $\times$100. Magnified view of the boxed region in *B* is shown. The area with cellular infiltrates is indicated with the green dotted line. *C*, Blood vessel formation in Colon-26 tumors injected with OBP-301. Frozen sections of the tumors were also probed with an Ab against CD31. Scale bar represents 50 μm, and magnification is a $\times$200. *D*, Tumor sections were obtained from SCID mice 14 days after final administration of OBP-301. Frozen sections of tumors were stained with H&E. Scale bar represents 100 μm, and magnification is at $\times$100 magnification.

OBP-301 on Colon-26 tumors; this antiangiogenic effect, however, could be partially inhibited in the presence of anti-IFN-γ mAb (Fig. 6). Treatment with control IgG1 had no effect on the antiangiogenic effects of OBP-301. These results suggest that IFN-γ may be one of the important factors for OBP-301 to inhibit angiogenesis in vivo.

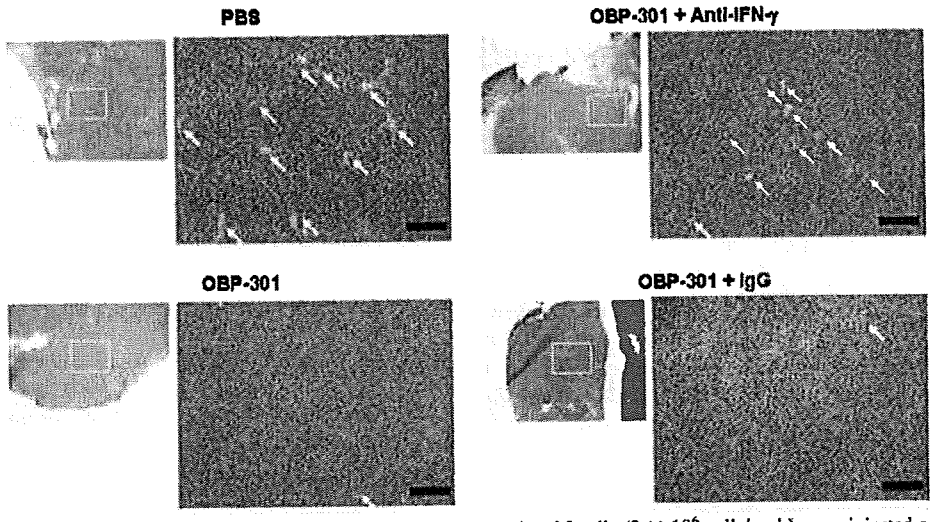

FIGURE 6. Effects of anti-IFN-γ Abs on angiogenesis in Colon-26 tumors. Colon-26 cells (2×10^6 cells/each) were injected s.c. into the right flank of syngenic BALB/c mice and OBP-301 (1×10^8 PFU/body) was administered intratumorally for three cycles every 2 days as described in Fig. 4. Mice were administered 200 μg of anti-IFN-γ mAb (XMG1.2) i.p. to neutralize IFN-γ 1 day before the first injection of OBP-301 and on days 1 and 3 after the first injection. Control mice received i.p. administration of isotype-matched rat IgG1 or PBS. Frozen sections of tumors obtained 14 days after final administration of OBP-301 were stained with H&E. Magnified view (*right*) of the boxed region (*left*). Microvessels are shown (arrow). Scale bar represents 50 μm, and magnification is at $\times$200.

Discussion

The tumor vasculature provides a new and attractive target for cancer therapy because of the reliance of most tumor cells on an adequate vascular supply for their growth and survival. Although the beneficial effects of novel antiangiogenic agents such as bevacizumab have been recently shown (15), regulation of endogenous antiangiogenic mediators may be another approach to inhibit angiogenesis. In the present study, we showed that OBP-301 infection and replication induced cytolysis of tumor cells with subsequent stimulation of host immune cells, which in turn inhibited tumor angiogenesis in vivo. Treatment of established murine colon tumors with intratumoral injection of OBP-301 resulted in a significant antitumor response characterized by extensive necrosis and reduced vascularity.

We reported previously that wild-type *p53* tumor suppressor gene transfer by a replication-deficient adenovirus vector (Advexin) could have antiangiogenic effects. The effects could be through down-regulation of angiogenic factor VEGF and up-regulation of antiangiogenic factor BAI1 because tumor p53 protein is a potent transcriptional factor (16, 17). In contrast, OBP-301 contains no therapeutic genes such as *p53* and, therefore, its infection may not directly influence the angiogenic property of infected tumor cells. However, because viral infection is known to trigger innate and adaptive immune responses presumably through the release of proinflammatory cytokines (18–20), local administration of OBP-301 might affect the tumor microenvironment, thus explaining the potential therapeutic benefit on tumor angiogenesis. In fact, dying tumor cells infected with OBP-301 promoted the production of Th1 cytokines by PBMC such as IFN-γ, which is one of the most potent antiangiogenic factors (21, 22) (Fig. 1). Viral infection itself has been reported to activate dendritic cells to secrete pro- or anti-inflammatory cytokines (23); our preliminary experiments, however, demonstrated that OBP-301 alone had no effect on cytokine production by PBMC (13), indicating that OBP-301 itself may be less infective or stimulatory to PBMC. The result is consistent with our previous finding that OBP-301 attenuated replication as well as cytotoxicity of human normal cells (9, 10). Moreover, OBP-301-infected tumor cells, but not untreated tumor cells, enhanced IFN-γ-inducible proteasome activator PA28 expression in the presence of PBMC (13), indicating that only dying tumor cells could trigger IFN-γ production by PBMC.

IFN-γ has been also known to inhibit tumor angiogenesis through the subsequent stimulation of secondary mediators, including monokine induced by IFN-γ and IFN-inducible protein 10 (24). Indeed, the observation that the supernatants of PBMC cocultured with OBP-301-infected human colorectal cancer cells exhibited a more profound antiangiogenic effect than recombinant IFN-γ (Fig. 2) suggests that other factors in addition to IFN-γ, which may not be related to IFN-γ, play important roles in inhibition of tumor cell-mediated angiogenesis. For example, we also found that oncolytic cells stimulated PBMC to secrete IL-12, which is an inducer of IFN-γ as well as an antiangiogenic factor, into the culture supernatants (13). The supernatants of neither virus-infected tumor cells alone nor PBMC alone were more antiangiogenic compared with those of MLTC in vivo (Fig. 3). Therefore, the interaction of oncolytic cells and PBMC is required to produce antiangiogenic mediators and to inhibit in vivo angiogenesis following OBP-301 treatment. The question what kind of cells produce mediators for antiangiogenic effects is of interest. We reported previously that OBP-301 replication produced the endogenous danger signaling molecule, uric acid, in infected human tumor cells, which in turn stimulated dendritic cells to produce IFN-γ as well as IL-12 into the supernatants (13). The amount of IFN-γ produced by dendritic cells was ~40 pg/ml, although 250 pg/ml IFN-γ was detected in the MLTC supernatants (Fig. 1*B*), indicating that other cell types may contribute to IFN-γ production. Lymphocytes that promote innate immunity (i.e., NK cells) as well as classical $CD4^+$ and $CD8^+$ T cells are also know to produce IFN-γ (25). Thus, dendritic cells represent one of the sources of IFN-γ; however, IL-12 secreted from dendritic cells activated with OBP-301-infected tumor cells might trigger these cells to produce IFN-γ.

To more directly evaluate the antiangiogenic effect of OBP-301, we used a syngenic BALB/c model established by s.c. inoculation of Colon-26 murine colon adenocarcinoma cells. OBP-301 is reported to have high infectivity and the potential to induce cell death in a variety of human cancer cells (9–12), whereas murine cells are relatively refractory to adenovirus infection due to the low expression of the coxsackievirus and adenovirus receptor. We have confirmed previously that telomerase-specific oncolytic adenovirus could infect and replicate in Colon-26 cells (12). Intratumoral administration of OBP-301 significantly inhibited the growth of Colon-26 tumors in syngenic immunocompetent BALB/c mice, although the magnitude of suppression was much less when compared with that in human tumor xenografts (9, 10). The finding that tumor growth suppression by OBP-301 was partially inhibited in immunodeficient SCID mice (Fig. 4) indicates that the host immune system could be partially responsible for the antitumor effect of OBP-301. Histopathologic analysis revealed that the presence of the immune cell infiltrates and the massive necrosis in Colon-26 tumors are exclusively due to the tumor-specific viral replication because dl312-injected tumors showed neither cellular infiltrates nor tissue damages (Fig. 5*B*). In view of the fact that a cellular infiltration could be still observed as late as 14 days after the last OBP-301 injection, immune responses are likely to be induced by oncolytic tumor cells. Furthermore, as expected, tumors injected with OBP-301 formed less blood vessels than mock- or dl312-treated tumors (Fig. 5, *B* and *C*), suggesting that inhibition of angiogenesis by infiltrating cell-secreted mediators partially elicits the antitumor activity of OBP-301. In contrast, antiangiogenic effect of OBP-301 was impaired in SCID mice (Fig. 5*D*), indicating that host immune cells are necessary for this function of OBP-301. Moreover, IFN-γ is considered to be partially responsible for the antiangiogenic effects of OBP-301 because in vivo neutralization of IFN-γ by anti-IFN-γ mAb increased angiogenesis on Colon-26 tumors (Fig. 6).

It remains to be studied whether OBP-301-infected oncolytic cells are capable of inhibiting the growth of distant tumors. Circulating inhibitors of angiogenesis such as angiostatin and endostatin can suppress the growth of remote metastases (26). The observation that none of mice treated with OBP-301 showed signs of viral distress (ruffled fur, weight loss, lethargy, or agitation) as well as histopathologic changes in any organs at autopsy (data not shown) suggests that the cytokine secretion by oncolytic cell-stimulated immune cells might be local rather than systemic. Thus, it is unlikely that locally produced antiangiogenic factors interfere with the distant tumor growth, although the circulating virus itself can infect and replicate in metastatic tumors. This question is being currently investigated in our laboratory.

In conclusion, we provide for the first time evidence that oncolytic virotherapy induces novel antiangiogenic effect by stimulating host immune cells to produce antiangiogenic mediators such as IFN-γ. Our data suggest that the antitumor effect of OBP-301 might be both direct and indirect.

Acknowledgments

We thank Hitoshi Kawamura and Daiju Ichimaru for helpful discussion. We also thank Yoshiko Shirakiya, Nobue Mukai, and Tomoko Sueishi for excellent technical assistance.

Disclosures

The authors have no financial conflict of interest.

References

1. Folkman, J. 1985. Tumor angiogenesis. *Adv. Cancer Res.* 43: 175–203.
2. Ausprunk, D. H., and J. Folkman. 1977. Migration and proliferation of endothelial cells in preformed and newly formed blood vessels during tumor angiogenesis. *Microvasc. Res.* 14: 53–65.
3. Fidler, I. J., and L. M. Ellis. 1994. The implications of angiogenesis for the biology and therapy of cancer metastasis. *Cell* 79: 85–88.
4. Folkman, J. 1995. Angiogenesis in cancer, vascular, rheumatoid and other disease. *Nat. Med.* 1: 27–31.
5. Hanahan, D., and J. Folkman. 1996. Patterns and emerging mechanisms of the angiogenesis switch during tumorgenesis. *Cell* 86: 353–364.
6. Nyberg, P., L. Xie, and R. Kalluri. 2005. Endogenous inhibitors of angiogenesis. *Cancer Res.* 65: 3967–3979.
7. de Visser, K. E., A. Eichten, and L. M. Coussens. 2006. Paradoxical roles of the immune system during cancer development. *Nat. Rev. Cancer* 6: 24–37.
8. Lin, W. W., and M. Karin. 2007. A cytokine-mediated link between innate immunity, inflammation, and cancer. *J. Clin. Invest.* 117: 1175–1183.
9. Kawashima, T., S. Kagawa, N. Kobayashi, Y. Shirakiya, T. Umeoka, F. Teraishi, M Taki, S. Kyo, N. Tanaka, and T. Fujiwara. 2004. Telomerase-specific replication-selective virotherapy for human cancer. *Clin. Cancer Res.* 10: 285–292.
10. Taki, M., S. Kagawa, M. Nishizaki, H. Mizuguchi, T. Hayakawa, S. Kyo, K. Nagai, Y. Urata, N. Tanaka, and T. Fujiwara. 2005. Enhanced oncolysis by a tropism-modified telomerase-specific replication-selective adenoviral agent OBP-405 ("Telomelysin-RGD"). *Oncogene* 24: 3130–3140.
11. Umeoka, T., T. Kawashima, S. Kagawa, F. Teraishi, M. Taki, M. Nishizaki, S. Kyo, K. Nagai, Y. Urata, N. Tanaka, and T. Fujiwara. 2004. Visualization of intrathoracically disseminated solid tumors in mice with optical imaging by telomerase-specific amplification of a transferred green fluorescent protein gene. *Cancer Res.* 64: 6259–6265.
12. Kishimoto, H., T. Kojima, Y. Watanabe, S. Kagawa, T. Fujiwara, F. Uno, F. Teraishi, S. Kyo, H. Mizuguchi, Y. Urata, et al. 2006. In vivo imaging of lymph node metastasis with telomerase-specific replication-selective adenovirus. *Nat. Med.* 12: 1213–1219.
13. Endo, Y., R. Sakai, M. Ouchi, H. Onimatsu, M. Hioki, S. Kagawa, F. Uno, Y. Watanabe, Y. Urata, N. Tanaka, and T. Fujiwara. 2008. Virus-mediated oncolysis induces danger signal and stimulates cytotoxic-T-lymphocyte activity via proteasome activator upregulation. *Oncogene* 27: 2375–2381.
14. Tanaka, N. G., N. Sakamoto, K. Inoue, H. Korenaga, S. Kadoya, H. Ogawa, and Y. Osada. 1989. Antitumor effects of an antiangiogenic polysaccharide from an *Arthrobacter* species with or without a steroid. *Cancer Res.* 49: 6727–6730.
15. Pfeiffer, P., C. Qvortrup, and J. G. Eriksen. 2007. Current role of antibody therapy in patients with metastatic colorectal cancer. *Oncogene* 26: 3661–3678.
16. Bouvet, M., L. M. Ellis, M. Nishizaki, T. Fujiwara, W. Liu, C. D. Bucana, B. Fang, J. J. Lee, and J. A. Roth. 1998. Wild-type p53 gene transfer down-regulates vascular endothelial growth factor expression and inhibits angiogenesis in human colon cancer. *Cancer Res.* 58: 2288–2292.
17. Nishizaki, M., T. Fujiwara, T. Tanida, A. Hizuta, H. Nishimori, T. Tokino, Y. Nakamura, M. Bouvet, J. A. Roth, and N. Tanaka. 1999. Recombinant adenovirus expressing wild-type p53 is antiangiogenic: a proposed mechanism for bystander effect. *Clin. Cancer Res.* 5: 1015–1023.
18. Lindenmann, J., and P. A. Klein. 1967. Viral oncolysis: increased immunogenicity of host cell antigen associated with influenza virus. *J. Exp. Med.* 126: 93–108.
19. Sinkovics, J. G. 1991. Viral oncolysates as human tumor vaccines. *Int. Rev. Immunol.* 7: 259–287.
20. Li, H., A. Dutuor, X. Fu, and X. Zhang. 2007. Induction of strong antitumor immunity by an HSV-2-based oncolytic virus in a murine mammary tumor model. *J. Gene Med.* 9: 161–169.
21. Fathallah-Shaykh, H. M., L. J. Zhao, A. I. Kafrouni, G. M. Smith, and J. Forman. 2000. Gene transfer of IFN-γ into established brain tumors represses growth by antiangiogenesis. *J. Immunol.* 164: 217–222.
22. Qin, Z., J. Schwartzkopff, F. Pradera, T. Kammertoens, B. Seliger, H. Pircher, and T. Blankenstein. 2003. A critical requirement of interferon γ-mediated angiostasis for tumor rejection by CD8$^-$ T cells. *Cancer Res.* 63: 4095–4100.
23. Ho, L. J., J. J. Wang, M. F. Shaio, C. L. Kao, D. M. Chang, S. W. Han, and J. H. Lai. 2001. Infection of human dendritic cells by Dengue virus causes cell maturation and cytokine production. *J. Immunol.* 166: 1499–1506.
24. Horton, M. R., C. M. McKee, C. Bao, F. Liao, J. M. Farber, J. Hodge-DuFour, E. Pure, B. L. Oliver, T. M. Wright, and P. W. Noble. 1998. Hyaluronan fragments synergize with interferon-γ to induce the C-X-C chemokines mig and interferon-inducible protein-10 in mouse macrophages. *J. Biol. Chem.* 273: 35088–35094.
25. Ikeda, H., L. J. Old, and R. D. Schreiber. 2002. The roles of IFN γ in protection against tumor development and cancer immunoediting. *Cytokine Growth Factor Rev.* 13: 95–109.
26. Folkman, J. 2002. Role of angiogenesis in tumor growth and metastasis. *Semin. Oncol.* 29: 15–18.

Telomerase-Specific Virotheranostics for Human Head and Neck Cancer

Yuji Kurihara,[1] Yuichi Watanabe,[2,3] Hideki Onimatsu,[2] Toru Kojima,[4] Tatsuo Shirota,[1] Masashi Hatori,[1] Dong Liu,[5] Satoru Kyo,[6] Hiroyuki Mizuguchi,[7] Yasuo Urata,[2] Satoru Shintani,[1] and Toshiyoshi Fujiwara[3,4]

Abstract **Purpose:** Long-term outcomes of patients with squamous cell carcinoma of the head and neck (SCCHN) remain unsatisfactory despite advances in combination of treatment modalities. SCCHN is characterized by locoregional spread and it is clinically accessible, making it an attractive target for intratumoral biological therapies.

Experimental Design: OBP-301 is a type 5 adenovirus that contains the replication cassette in which the human telomerase reverse transcriptase promoter drives expression of the *E1* genes. OBP-401 contained the replication cassette and the green fluorescent protein (*GFP*) gene. The antitumor effects of OBP-301 were evaluated *in vitro* by the sodium 30-[1-(phenylaminocarbonyl)-3,4-tetrazolium]-bis(4-methoxy-6-nitro)benzene sulfonic acid hydrate assay and *in vivo* in an orthotopic xenograft model. Virus spread into the lymphatics was also orthotopically assessed by using OBP-401.

Results: Intratumoral injection of OBP-301 resulted in the shrinkage of human SCCHN tumors orthotopically implanted into the tongues of BALB/c *nu/nu* mice and significantly recovered weight loss by enabling oral ingestion. The levels of GFP expression following *ex vivo* infection of OBP-401 may be of value as a positive predictive marker for the outcome of telomerase-specific virotherapy. Moreover, whole-body fluorescent imaging revealed that intratumorally injected OBP-401 could visualize the metastatic lymph nodes, indicating the ability of the virus to traffic to the regional lymphatic area and to selectively replicate in neoplastic lesions, resulting in GFP expression and cell death in metastatic lymph nodes.

Conclusions: These results illustrate the potential of telomerase-specific oncolytic viruses for a novel therapeutic and diagnostic approach, termed theranostics, for human SCCHN.

Cancer remains a leading cause of death worldwide despite improvements in diagnostic techniques and clinical management (1, 2). An estimated 500,000 patients worldwide are diagnosed with squamous cell carcinoma of the head and neck (SCCHN) annually. This aggressive epithelial malignancy is associated with a high mortality rate and severe morbidity among the long-term survivors (3). Current treatment strategies for advanced SCCHN include surgical resection, radiation, and cytotoxic chemotherapy. Although a combination of these modalities can improve survival, most patients eventually experience disease progression that leads to death; disease progression is often the result of intrinsic or acquired resistance to treatment (4, 5). A lack of specificity for tumor cells is the primary limitation of radiotherapy and chemotherapy. To improve the therapeutic index, there is a need for anticancer agents that selectively target only tumor cells and spare normal cells.

Replication-selective tumor-specific viruses present a novel approach for cancer treatment (6, 7). We reported previously that telomerase-specific replication-competent adenovirus (OBP-301, Telomelysin), in which the human telomerase reverse transcriptase (hTERT) promoter element drives the expression of *E1A* and *E1B* genes linked with an IRES, induced selective E1 expression, and efficiently killed human cancer cells but not normal cells (8–10). We also found that intratumoral injection of telomerase-specific replication-selective adenovirus expressing the green fluorescent protein (*GFP*) gene (OBP-401, TelomeScan) causes viral spread into the regional lymphatic area with subsequent selective replication in

Authors' Affiliations: [1]Department of Oral and Maxillofacial Surgery, School of Dentistry, Showa University and [2]Oncolys BioPharma, Inc., Tokyo, Japan; [3]Center for Gene and Cell Therapy, Okayama University Hospital and [4]Division of Surgical Oncology, Department of Surgery, Okayama University Graduate School of Medicine, Dentistry and Pharmaceutical Sciences, Okayama, Japan; [5]Research Center of Lung Cancer, Shanghai Pulmonary Hospital, Shanghai, China; [6]Department of Obstetrics and Gynecology, Kanazawa University School of Medicine, Kanazawa, Japan; and [7]Department of Biochemistry and Molecular Biology, Graduate School of Pharmaceutical Sciences, Osaka University, Osaka, Japan

Received 10/22/08; revised 12/17/08; accepted 12/31/08; published OnlineFirst 3/24/09.

Grant support: Grants-in-Aid from the Ministry of Education, Science, and Culture, Japan (T. Fujiwara), and Grants from the Ministry of Health and Welfare, Japan (T. Fujiwara).

The costs of publication of this article were defrayed in part by the payment of page charges. This article must therefore be hereby marked *advertisement* in accordance with 18 U.S.C. Section 1734 solely to indicate this fact.

Note: Supplementary data for this article are available at Clinical Cancer Research Online (http://clincancerres.aacrjournals.org/).

Requests for reprints: Toshiyoshi Fujiwara, Center for Gene and Cell Therapy, Okayama University Hospital, 2-5-1 Shikata-cho, Okayama 700-8558, Japan. Phone: 81-86-235-7997; Fax: 81-86-235-7884; E-mail: toshi_f@md.okayama-u.ac.jp.

doi:10.1158/1078-0432.CCR-08-2690

Translational Relevance

Despite new therapeutic modalities, long-term outcomes of patients with squamous cell carcinoma of the head and neck (SCCHN) remain unsatisfactory. Thus, the development of efficient treatment methods to enable the reduction of tumors in these patients is clearly imperative. Tumor-targeted oncolytic viruses have the potential to selectively infect target tumor cells, multiply, and cause cell death and release of viral particles, leading to the spread of viral-mediated antitumor effects. We developed a telomerase-specific oncolytic adenovirus OBP-301 (Telomelysin) as well as OBP-401 – expressing *GFP* gene (TelomeScan). Our data showed that telomerase-specific oncolytic viruses can be effective to kill human SCCHN cells *in vitro* and *in vivo* as well as to identify the patients who will likely benefit from virotherapy, suggesting that an oncolytic virus-based approach exhibited desirable features of a novel "virotheranostics," the combination of a diagnostic assay with a therapeutic entity for human SCCHN. This is a preclinical study for the future clinical trials.

metastatic lymph nodes in *nu/nu* mice (11). Although up to 25% of patients with SCCHN develop distant metastasis to the lung, liver, or bone, lymph node metastases are more common in SCCHN patients (12); therefore, locoregional disease control with telomerase-specific oncolytic viruses may be a novel therapeutic strategy that is clinically applicable for the treatment of human SCCHN.

In the present study, we explore the therapeutic as well as diagnostic ability of telomerase-specific oncolytic viruses *in vitro* and *in vivo*. To this end, we adopted an orthotopic head and neck cancer xenograft model by inoculating human SCCHN cells into the tongues of *nu/nu* mice; this model resembles human SCCHN in a number of biological properties (13).

Materials and Methods

Cell lines and cell culture. The human oral squamous carcinoma cell lines SAS-L, SCC-4, SCC-9, HSC-2, HSC-3, and HSC-4 were maintained *in vitro* as monolayers in DMEM supplemented with 10% heat-inactivated fetal bovine serum, 100 units/mL penicillin, and 100 mg/mL streptomycin (complete medium). The human non–small-cell lung cancer cell line H460 and the human esophageal cancer cell line TE8 were routinely propagated in monolayer culture in RPMI 1640 supplemented with 10% fetal bovine serum. The normal human lung diploid fibroblast cell line WI38 (JCRB0518) was obtained from the Health Science Research Resources Bank (Osaka, Japan) and grown in Eagle's MEM with 10% fetal bovine serum. The normal human lung fibroblast NHLF (TaKaRa Biomedicals) and the normal human embryonic lung fibroblast MRC-5 (RIKEN BioResource Center) were cultured according to the vendors' specifications.

Adenoviruses. The recombinant replication-selective, tumor-specific adenovirus vector OBP-301 (Telomelysin), in which the hTERT promoter element drives the expression of *E1A* and *E1B* genes linked with an IRES, was previously constructed and characterized (8–10). OBP-401 is a telomerase-specific replication-competent adenovirus variant with the replication cassette, and *GFP* gene under the control of the cytomegalovirus promoter was inserted into the E3 region for monitoring viral replication (11, 14). The viruses were purified by ultracentrifugation in cesium chloride step gradients, their titers were determined by a plaque-forming assay using 293 cells, and they were stored at -80°C.

Cell viability assay. An sodium 30-[1-(phenylaminocarbonyl)-3,4-tetrazolium]-bis(4-methoxy-6-nitro)benzene sulfonic acid hydrate (XTT) assay was done to assess the viability of tumor cells. Human SCCHN cells (1,000 per well) were seeded onto 96-well plates 18 to 20 h before viral infection. Cells were then infected with OBP-301 at a multiplicity of infection (MOI) of 1, 10, 50, and 100 plaque-forming units (pfu) per cell. Cell viability was determined at the indicated time points by using a Cell Proliferation Kit II (Roche Molecular Biochemicals) according to the protocol provided by the manufacturer.

Fluorescence microplate reader. Cells were infected with OBP-401 at the indicated MOI values in a 96-well black-bottomed culture plate and further incubated for the indicated time periods. GFP fluorescence was measured by using a fluorescence microplate reader (DS Pharma Biomedical) with excitation/emission at 485 nm/528 nm.

Animal experiments. SAS-L and HSC-3 human oral squamous cell carcinoma cells were harvested and suspended at a concentration of 5×10^6/mL in the medium. To generate an orthotopic head and neck cancer model, 6-wk-old female BALB/c *nu/nu* mice were anesthetized and injected directly with 20 μL of cell suspension at a density of 10^5 cells. The cells were injected into the right lateral border of the tongue with a 27-gauge needle. When the tumor grew to 2 to 3 mm in diameter ~5 to 7 days later, 20 μL of solution containing 1×10^8 pfu of OBP-301, OBP-401, or PBS were injected into the tumor. The perpendicular diameter of each tumor was measured every 3 d, and tumor volume was calculated by using the following formula: tumor volume (mm^3) = $a \times b^2 \times 0.5$, where a is the longest diameter, b is the shortest diameter, and 0.5 is a constant to calculate the volume of an ellipsoid. The body weights of mice were monitored and recorded. The experimental protocol was approved by the Ethics Review Committee for Animal Experimentation of Okayama University.

In vivo *fluorescence imaging.* *In vivo* GFP fluorescence imaging was acquired by illuminating the animal with a Xenon 150-W lamp. The reemitted fluorescence was collected through a long-pass filter on a Hamamatsu C5810 3-chip color charge-coupled device camera (Hamamatsu Photonics Systems). High-resolution image acquisition was accomplished by using an EPSON PC. Images were processed for contrast and brightness with the use of Adobe Photoshop 4.0.1J software (Adobe). A fluorescence stereomicroscope (SZX7; Olympus) was also used to visualize GFP-positive tissues.

Statistical analysis. The statistical significance of the differences in the *in vitro* and *in vivo* antitumor effects of viruses was determined by using the Student's t test (two-tailed). The antitumor effect viruses on orthotopically implanted tumors in nude mice were assessed by plotting survival curves according to the Kaplan-Meier method. P values <0.05 were considered statistically significant.

Results

In vitro *cytopathic efficacy of OBP-301 on human SCCHN cell lines.* We examined the cytopathic effect of OBP-301, which is an attenuated adenovirus in which the hTERT promoter element drives expression of *E1A* and *E1B* genes linked with an internal ribosome entry site (IRES; Fig. 1A), on various human SCCHN cell lines by the XTT cell viability assay. OBP-301 infection induced cell death in human SCCHN cells in a dose-dependent manner; the sensitivity, however, varied among different cell lines (Fig. 1B). The ID_{50} values calculated from the dose-response curves confirmed that SAS-L cells could be efficiently killed by OBP-301 at an multiplicity of infection (MOI) of <150 (ID_{50} = 148), whereas HSC-3 cells were less sensitive to OBP-301 (ID_{50} = 500; Fig. 1C).

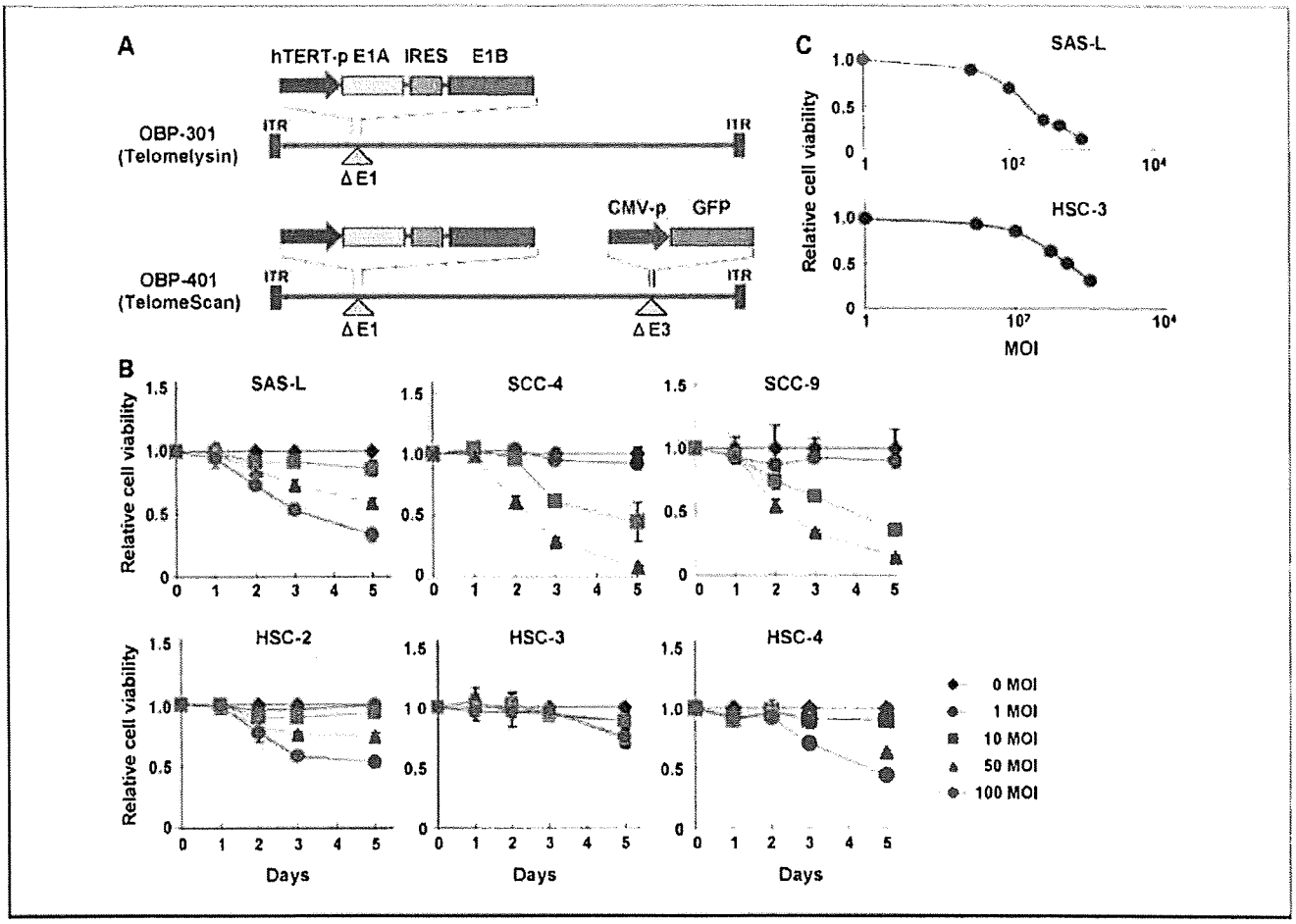

Fig. 1. Schematic DNA structures of telomerase-specific viruses and selective cytopathic effect in human SCCHN cell lines *in vitro*. *A*, OBP-301 is a telomerase-specific replication-competent adenovirus containing the hTERT promoter sequence inserted into the adenovirus genome to drive transcription of the E1A and E1B bicistronic cassette linked by the IRES. OBP-401 is a variant of OBP-301, in which the *GFP* gene is inserted under the cytomegalovirus (*CMV*) promoter into the E3 region for monitoring viral replication. *B*, human SCCHN cell lines were infected with OBP-301 at the indicated MOI values, and surviving cells were quantitated over 5 d by the XTT assay. The cell viability of mock-treated cells on day 0 was considered 1.0, and the relative cell viability was calculated. Points, mean of triplicate experiments; bars, SD. *C*, effects of various concentrations of OBP-301 on SAS-L and HSC-3 cells assessed 5 d after the XTT assay. Results are expressed as the relative cell viability of untreated control cells.

To confirm the specificity of telomerase activity in human SCCHN cells, we next measured the expression of *hTERT* mRNA in a panel of human SCCHN cell lines and normal cell lines by using a real-time reverse transcription-PCR method. Although the levels of expression varied widely, all SCCHN cell lines expressed detectable levels of *hTERT* mRNA, whereas human fibroblast cells such as NHLF and WI38 were negative for *hTERT* expression (Supplementary Fig. S1A). We also examined the expression levels of coxsackievirus and adenovirus receptor on the cell surface of each type of cell by flow cytometric analysis. Apparent amounts of coxsackievirus and adenovirus receptor expression were detected on SAS-L and HSC-3 human SCCHN cells (Supplementary Fig. S1B).

To assess whether viral replication was restricted to tumor cells, we next examined the replication ability of OBP-301 by measuring the relative amounts of E1A DNA. SAS-L human SCCHN cells and MRC-5 human fibroblasts were harvested at indicated time points over 72 h after infection with OBP-301 and subjected to quantitative real-time PCR analysis. The ratios were normalized by dividing the value of cells obtained 2 h after viral infection. OBP-301 replicated 3 to 4 logs within 48 h after infection; the viral replication, however, was attenuated up to 2 logs in normal MRC-5 cells (Supplementary Fig. S2).

The response of tumor cells to DNA-damaging stimuli such as chemotherapeutic drugs and ionizing radiation is predetermined by the functional status of their *p53* gene (15); however, the p53 status of human SCCHN cell lines (wild-type p53 [SAS-L], mutant p53 [SCC-4, HSC-2, HSC-3, HSC-4], and deleted p53 [SCC-9]) is not related to their sensitivity to OBP-301. Indeed, OBP-301 similarly killed parental SAS-L cells and cells stably transfected with the mutant *p53* gene (Supplementary Fig. S3), suggesting that OBP-301 induces cell death in a p53-independent manner.

Selective replication of OBP-401 in human SCCHN cell lines in vitro. OBP-401 is a genetically engineered adenovirus that expresses GFP by inserting the *GFP* gene under the control of the cytomegalovirus promoter at the deleted E3 region of OBP-301 (Fig. 1A). To determine whether OBP-401 replication is associated with selective GFP expression in human SCCHN cells, cells were analyzed and recorded by using a time-lapse fluorescent microscope after OBP-401 infection. Representative images at the indicated time points are shown (Fig. 2A). SAS-L

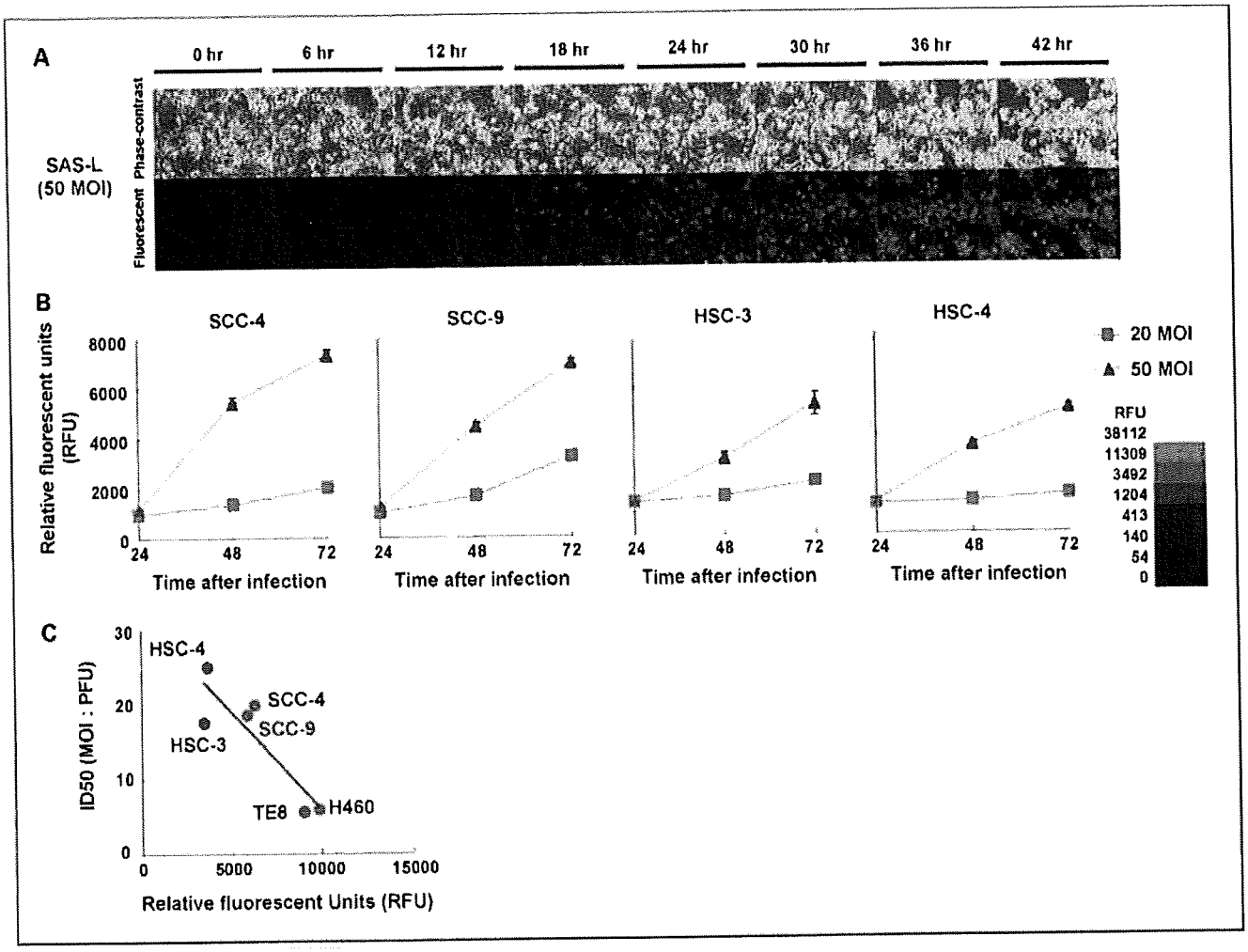

Fig. 2. Selective visualization of human SCCHN cells *in vitro* by OBP-401. *A*, time-lapse images of SAS-L cells were recorded for 42 h after OBP-401 infection at a MOI of 50. Representative images taken at the indicated time points show cell morphology by phase-contrast microscopy (*top*) and GFP expression under fluorescence microscopy (*bottom*). Magnification, ×200. *B*, quantitative assessment of GFP labeling by OBP-401 in human SCCHN cell lines. Cells were infected with OBP-401 at the indicated MOI values, and GFP fluorescence was measured over 72 h by the fluorescence microplate reader. The intensity of green fluorescence was evaluated based on the brightness determinations used as relative fluorescence units (*RFU*). The relative fluorescence unit and time after infection were plotted on the ordinate and abscissa, respectively. A green color calibration bar for the indicated relative fluorescence unit is shown on the right. *C*, relationship between GFP fluorescence after OBP-401 infection and ID_{50} values after OBP-301 infection in human cancer cell lines, including SCCHN cells. Relative GFP fluorescence was measured by the fluorescence microplate reader 72 h after OBP-401 infection at a MOI of 50. The ID_{50} values of OBP-301 on cell viability at 5 d after infection were calculated and expressed as ID_{50} values. The slope represents the inverse correlation between these two factors ($R^2 = 0.7839$).

human SCCHN cells expressed bright GFP fluorescence as early as 12 h after OBP-401 infection at a MOI of 50. The fluorescence intensity gradually increased in a dose-dependent manner, followed by rapid cell death due to the cytopathic effect of OBP-401, as evidenced by floating, highly light-refractile cells under phase-contrast photomicrographs.

We also quantified GFP expression in human SCCHN cells following OBP-401 infection by using a fluorescence plate reader. Relative expression levels of GFP gradually increased in a dose-dependent manner (Fig. 2B). Moreover, we found an apparent inverse correlation between relative GFP expression at 72 h after OBP-401 infection and the ID_{50} values of OBP-301 in various human cancer cell lines including SCCHN cell lines (Fig. 2C), indicating that the outcome of OBP-301 treatment could be predicted by measuring GFP expression following OBP-401 infection.

In vivo *antitumor effect of intratumoral injection of OBP-301 in an orthotopic nude mouse model of human SCCHN.* To assess the effect of OBP-301 on SCCHN *in vivo*, we used an orthotopic animal model for SCCHN in which SAS-L cells were implanted into the tongues of BALB/c *nu/nu* mice. Histopathologic examination of the excised primary tumors showed a tumor formation composed of implanted SAS-L cells with a solid architecture (Fig. 3A). Mice bearing palpable SAS-L tumors with a diameter of 3 to 5 mm received three courses of intratumoral injections of 10^8 pfu of OBP-301 or PBS (mock treatment) every 3 days beginning on the 7th day (regimen 1) or 10th day (regimen 2) after the initial tumor inoculation (Fig. 3B). Representative images from each group showed that tumors treated with OBP-301 starting on day 7 after tumor inoculation were consistently smaller than those of mock-treated mice 28 days after the first viral injection (Fig. 3C).